Dalton Transactions

Accepted Manuscript

This is an *Accepted Manuscript*, which has been through the Royal Society of Chemistry peer review process and has been accepted for publication.

Accepted Manuscripts are published online shortly after acceptance, before technical editing, formatting and proof reading. Using this free service, authors can make their results available to the community, in citable form, before we publish the edited article. We will replace this *Accepted Manuscript* with the edited and formatted *Advance Article* as soon as it is available.

You can find more information about *Accepted Manuscripts* in the Information for Authors.

Please note that technical editing may introduce minor changes to the text and/or graphics, which may alter content. The journal's standard Terms & Conditions and the Ethical guidelines still apply. In no event shall the Royal Society of Chemistry be held responsible for any errors or omissions in this *Accepted Manuscript* or any consequences arising from the use of any information it contains.

ROYAL SOCIETY OF CHEMISTRY

www.rsc.org/dalton

Electronic structures and selective fluoride sensing features of $Os(bpy)_2(HL^{2-})$ and $[\{Os(bpy)_2\}_2(\mu\text{-}HL^{2-})]^{2+}$ (H_3L: 5-(1*H*-benzo[*d*]imidazol-2-yl)-1*H*-imidazole-4-carboxylic acid)

Ankita Das,[a] Hemlata Agarwala,[a] Tanaya Kundu,[a] Prabir Ghosh,[a] Sudipta Mondal,[a] Shaikh M Mobin,[b] and Goutam Kumar Lahiri*[a]

[a]*Department of Chemistry, Indian Institute of Technology Bombay, Powai, Mumbai-400076, India. E-mail: lahiri@chem.iitb.ac.in*

[b]*Discipline of Chemistry, School of Basic Sciences, Indian Institute of Technology Indore, Indore 452017, India*

†Electronic supplementary information (ESI) available: X-ray crystallographic file for **1** in CIF format, crystal data for [**2**]$(Cl)_2$ (Tables S1 and S2), DFT dataset for $\mathbf{1}^n$ and $\mathbf{2}^n$ (Tables S3-S11, Fig. S2), NBO table (Table S12), mass spectra of **1**, [**2**]$(Cl)_2$ and [**2**]$(ClO_4)_2$ (Fig. S1), ORTEP plot of the cation of [**2**]$(Cl)_2$ (Fig. S3), visual change in colour of $\mathbf{2}^{2+}$ on addition of anions (Fig. S4), spectral changes of $\mathbf{2}^{2+}$ on addition of anions (Fig. S5), spectral changes of $\mathbf{2}^{2+}$ on addition of TBAF (Fig.S6), plots of change in absorbance of **1**/[**2**]$(ClO_4)_2$ with TBAF (Fig. S7), spectral changes of **1**/[**2**]$(ClO_4)_2$ with TBOH (Fig. S8), ^{1}H-NMR titration of $\mathbf{2}^{2+}$ with TBAF (Fig. S9), ^{19}F-NMR of TBAF in presence of **1** and [**2**]$(ClO_4)_2$ (Fig. S10), mass spectra of [**1**+2H+F^-] and [$\mathbf{2}^{2+}$+F^-] (Fig. S11). CCDC nos. 1008800 (**1**).

Dalton Transactions Accepted Manuscript

Abstract

The article deals with the newly designed mononuclear and asymmetric dinuclear osmium(II) complexes $Os^{II}(bpy)_2(HL^{2-})$ (**1**) and $[(bpy)_2Os^{II}(\mu\text{-}HL^{2-})Os^{II}(bpy)_2](Cl)_2$ ([**2**](Cl)$_2$) / $[(bpy)_2Os^{II}(\mu\text{-}HL^{2-})Os^{II}(bpy)_2](ClO_4)_2$ ([**2**](ClO$_4$)$_2$), respectively, (H_3L=5-(1*H*-benzo[*d*]imidazol-2-yl)-1*H*-imidazole-4-carboxylic acid and bpy=2,2′-bipyridine). The identity of **1** has been established by its single crystal X-ray structure. The ligand (HL^{2-}) based primary oxidation process (E^0_{298}, 0.23 V *versus* SCE) along with partial metal contribution (~20%) in **1** has been revealed by the ligand dominated HOMO of **1** (HL^{2-}: 88 %, Os: 8 %) as well as Mulliken spin density distribution of $\mathbf{1}^+$ (HL^{2-}: 0.878, Os: 0.220). Accordingly, $\mathbf{1}^+$ exhibits a free radical type EPR at 77 K with partial metal based anisotropic feature (g_1=2.127, g_2=2.096, g_3=2.046; $\langle g\rangle$=2.089; Δg=0.08). ^{1}H-NMR of the dinuclear $\mathbf{2}^{2+}$ in $CDCl_3$ suggests an intimate mixture of two diastereomeric forms in 1:1 ratio. The DFT supported predominantly Os(II)/Os(III) based couples of asymmetric $\mathbf{2}^{2+}$ at 0.24 V and 0.50 V *versus* SCE result in comproportionation constant (K_c) value of 8.2x10^4. The class I mixed valent state of $\mathbf{2}^{3+}$ (S=1/2) has however been corroborated by the Mulliken spin density distribution of Os1:0.887, Os2:0.005, HL^{2-}: 0.117 as well as by the absence of low-energy IVCT (intervalence charge transfer) band in the near-IR region (up to 2000 nm). Appreciable spin accumulation on the bridge in $\mathbf{2}^{3+}$ or $\mathbf{2}^{4+}$ (S=1, Os1: 0.915, Os2: 0.811 and HL^{2-}: 0.275) implies a mixed electronic structural form of $[(bpy)_2Os^{III}(\mu\text{-}HL^{2-})Os^{II}(bpy)_2]^{3+}$(major)/$[(bpy)_2Os^{II}(\mu\text{-}HL^{\bullet-})Os^{II}(bpy)_2]^{3+}$(minor) or $[(bpy)_2Os^{III}(\mu\text{-}HL^{2-})Os^{III}(bpy)_2]^{4+}$(major)/$[(bpy)_2Os^{III}(\mu\text{-}HL^{\bullet-})Os^{II}(bpy)_2]^{4+}$ (minor), respectively. The mixed valent $\{Os^{III}(\mu\text{-}HL^{2-})Os^{II}\}$ state in $\mathbf{2}^{3+}$ however fails to show EPR at 77 K due to the rapid spin relaxation process. The DFT supported bpy based two reductions for both $\mathbf{1}^+$ and $\mathbf{2}^{2+}$ appear in

Dalton Transactions Accepted Manuscript

the potential range of -1.5 V to -1.8 V *versus* SCE. The electronic transitions in $\mathbf{1}^{n}$ and $\mathbf{2}^{n}$ are assigned by TD-DFT calculations. Further, the potential anion sensing features of **1** and $\mathbf{2}^{2+}$ *via* the involvement of the available N-H proton in the framework of coordinated HL^{2-} have been evaluated by different experimental investigations in conjunction with DFT calculations using a wide variety of anions such as F^{-}, Cl^{-}, Br^{-}, I^{-}, OAc^{-}, SCN^{-}, HSO_4^{-} and $H_2PO_4^{-}$. It however establishes that both **1** and $\mathbf{2}^{2+}$ are equally efficient in recognising F^{-} ion selectively with log *K* values of 6.83 and 5.89, respectively.

Dalton Transactions Accepted Manuscript

Introduction

The discovery of strong intermetallic electronic coupling at the mixed valent $Ru^{II}Ru^{III}$ (d^6d^5) state in Creutz-Taube ion $[(NH_3)_5Ru^{II}(\mu\text{-pyrazine})Ru^{III}(NH_3)_5]^{5+}$ [1] has spurred the development of a wide variety of diruthenium[2-5] and to some extent analogous diosmium[2d,6] complexes. The primary research activities are centred around the understanding of the fundamental issues involving the mixed valent chemistry as well as to explore their potential applications in information transfer[7] and energy-relevant research.[8] In this context the detailed investigations on molecular frameworks encircling varying bridging and ancillary ligands (π-accepting as well as σ or π-donating) have revealed the effective role of both the bridging and ancillary ligands in tuning the intermetallic coupling process at the mixed valent state.[5e,9,10] Further, the presence of redox non-innocent bridging or ancillary ligand in such molecular frameworks introduces the initial challenging scenario of establishing the involvement of metal or bridge or mixed metal/bridge based orbitals in the electron-transfer processes. This often commences alternate electronic structural forms along the redox chain including radical bridged isovalent metal ions or radical bridged mixed valent metal ions instead of conventional mixed valent situation.[9,11]

Though mixed valent ruthenium compounds have been extensively scrutinised, studies on the corresponding osmium derivatives are rather limited.[2d,6] The mixed valent osmium complexes generally exhibit more complex electronic spectra and faster relaxation process leading to the EPR silent situation primarily due to stronger spin-orbit coupling effect (spin-orbit coupling constant λ/cm^{-1}: Os^{III}, 3000; Ru^{III}, 1000).[12]

The present article originates from our interest in exploring the osmium chemistry of the recently introduced structurally characterised[13] potential non-innocent ligand framework 5-(1*H*-

Dalton Transactions Accepted Manuscript

benzo[*d*]imidazol-2-yl)-1*H*-imidazole-4-carboxylic acid (H_3L) incorporating multiple dissociable N-H protons and it also has the prospective to bridge the metal fragments in unsymmetrical fashion.[14]

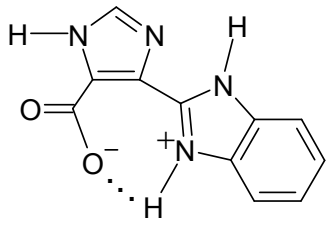

H_3L

Herein we report the synthesis, characterisation and electronic structural aspects of newly designed mononuclear and dinuclear osmium-bipyridine complexes incorporating partially deprotonated dianionic HL^{2-}, $[Os^{II}(bpy)_2(HL^{2-})]^n$ (**1**^{n}) and $[(bpy)_2Os^{II}(\mu\text{-}HL^{2-})Os^{II}(bpy)_2]^n$ (**2**^{n}). Moreover, the potential application of both **1** and $\mathbf{2}^{2+}$ encompassing one free NH function in the framework of coordinated HL^{2-} towards the selective recognition of anion(s) such as F^-, Cl^-, Br^-, I^-, OAc^-, HSO_4^-, $H_2PO_4^-$ and SCN^- has been explored *via* different experimental investigations and DFT calculations.

It should be noted that the selective recognition of anions by the suitably designed metal complex frameworks[15] has been considered to be important as anions play an important role in biological, industrial, and environmental processes.[16]

Dalton Transactions Accepted Manuscript

Results and discussion

Synthesis and characterisation

The heteroleptic mononuclear osmium complex $Os^{II}(bpy)_2(HL^{2-})$ (**1**) has been prepared from the preformed ligand H_3L (H_3L=5-(1*H*-benzo[*d*]imidazol-2-yl)-1*H*-imidazole-4-carboxylic acid) and the metal precursor, $Os^{II}(bpy)_2Cl_2$ (bpy=2,2′-bipyridine) in the presence of NEt_3 as a base in refluxing ethanol-water (2:1) mixture followed by chromatographic purification using a neutral alumina column. The unsymmetrical HL^{2-} bridged dinuclear complex $[(bpy)_2Os^{II}(\mu\text{-}HL^{2-})Os^{II}(bpy)_2](Cl)_2$ ([**2**](Cl)$_2$) has been obtained by reacting the precursor mononuclear complex (**1**) with one mole of $Os^{II}(bpy)_2Cl_2$ in refluxing ethanol-water (2:1) mixture. The perchlorate salt [**2**](ClO$_4$)$_2$ has been prepared from [**2**](Cl)$_2$ by chloride exchange process using saturated $NaClO_4$ solution and purified by column chromatography on a neutral alumina column (Scheme1, Experimental).

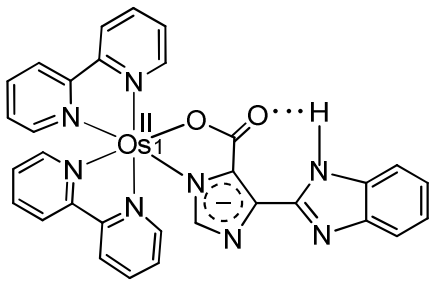

1

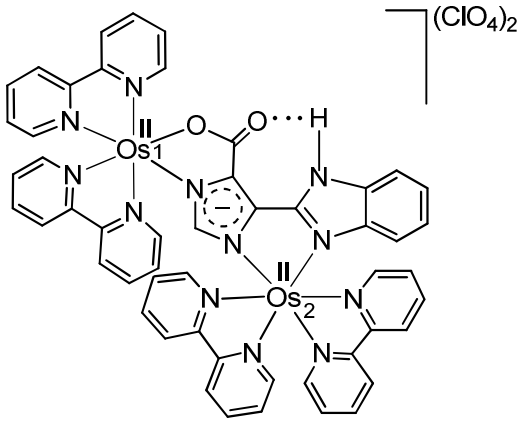

[**2**](ClO$_4$)$_2$

Scheme 1 Representation of complexes.

The identities of **1**, [**2**](Cl)$_2$ and [**2**](ClO$_4$)$_2$ have been confirmed by their mass spectral data in CH_3CN which exhibit molecular ion peaks at *m/z* 731.14, 1266.89 and 1330.72 corresponding to

Dalton Transactions Accepted Manuscript

$\{\mathbf{1}+H\}^+$ (calcd. 731.17), $\{[\mathbf{2}]Cl\}^+$ (calcd. 1266.79) and $\{[\mathbf{2}]ClO_4\}^+$ (calcd. 1330.79), respectively (Fig. S1†). The electrically neutral **1** and 1:2 conducting $[\mathbf{2}](Cl)_2$ or $[\mathbf{2}](ClO_4)_2$ give satisfactory microanalytical data (Experimental). The ν(C=O) vibrations of the coordinated HL^{2-} in **1**, $[\mathbf{2}](Cl)_2$ and $[\mathbf{2}](ClO_4)_2$ at 1625 cm^{-1},1621 cm^{-1} and 1619 cm^{-1}, respectively, are close to that of the free ligand (H_3L) value of 1627 cm^{-1}.[13] The ν(ClO_4) frequencies of $[\mathbf{2}](ClO_4)_2$ appear at 1100 cm^{-1} and 600 cm^{-1}. The expected N-H vibration of the coordinated HL^{2-} in the complexes could not be clearly identified due to the presence of a broad water peak (KBr disk) around the region of 3500-3300 cm^{-1}.

The crystal structure of **1** is shown in Fig. 1 and the selected crystallographic and bond parameters are listed in Tables 1 and 2. The doubly deprotonated unsymmetrical HL^{2-} in $Os^{II}(bpy)_2(HL^{2-})$ is selectively coordinated to the $\{Os(bpy)_2\}^{2+}$ unit through the anionic carboxylate oxygen (O1) and N1 donor of the imidazole moiety, forming a five membered chelate with a bite angle of 77.47(8)°. The Os1-N1(imidazole) and Os1-O1(carboxylate) bond lengths involving HL^{2-} in **1** of 2.059(2) Å and 2.116(18) Å, respectively, are close to earlier reported Ru-N(imidazole): 2.049(5) Å/2.054(4) Å and Ru-O(carboxylate): 2.102(4) Å/2.103(3) Å bond lengths for the corresponding $[Ru^{II}(bpy)_2(H_2L^-)]ClO_4$/$[Ru^{II}(bpy)_2(HL^{2-})]$, respectively.[13] The Os1-N1(imidazole) and Os1-O1(carboxylate) bond lengths in **1** also match well with the reported $\{Os^{II}(bpy)_2\}$ complexes incorporating partially deprotonated 4,5-bis(benzimidazol-2-yl)imidazole ligand.[17] The average Os-N(bpy) bond length of 2.038(8) Å in **1** matches reasonably well with the reported distances in analogous complexes.[17*b*,18] The bite angles involving HL^{2-} (N1-Os1-O1) and bpy (N6-Os1-N5/N8-Os1-N7) of 77.47(8)° and 78.27(8)°/78.76(8)°, respectively, and the *trans*-angles of N6-Os1-N1, 173.04(8)°; N8-Os1-N5, 173.49(8)°; N7-Os1-

Dalton Transactions Accepted Manuscript

O1, 171.66(7)° collectively imply a distorted octahedral geometry around the osmium(II) ion in **1**.

The crystal structure of **1** displays intramolecular N-H···O hydrogen bonding interaction involving the benzimidazole hydrogen atom, N4-H4 and the uncoordinated carboxylate oxygen atom (O2) (Fig. 1), where the H4···O2, N4-O2, N4-H4 distances and N4-H4···O2 angle are 1.983 Å, 2.783 Å, 0.881 Å and 150.35 ^{o}, respectively.

The DFT calculated bond parameters of **1** match fairly well with the experimental values (Fig. S2† and Table 2).

In spite of all our attempts we failed to generate the suitable single crystal of [**2**]$(ClO_4)_2$. Structure determination of [**2**]$(Cl)_2$ was attempted, however, it did not succeed owing to the bad crystal quality. The resulting connectivity study has been shown in Fig. S3† (Tables S1-S2†).

The ^{1}H-NMR spectrum of **1** in $CDCl_3$ (Fig. 10) exhibits partially overlapping aromatic proton resonances in the chemical shift range δ, 9-6.5 ppm corresponding to calculated number of twenty one aromatic protons in addition to one NH signal. The distinctly identifiable two singlets for the benzimidazole NH proton (D_2O exchangeable) and imidazole CH proton of coordinated HL^{2-} appear at δ, 13.93 ppm and 6.60 ppm, respectively. On the other hand, ^{1}H-NMR of [**2**]$(ClO_4)_2$ or [**2**]$(Cl)_2$ in $CDCl_3$ (Fig. S9†) shows two pairs of singlets in the ratio of 1:1 corresponding to the benzimidazole NH (D_2O exchangeable, δ: 11.78 and 11.65) ppm) and imidazole CH (δ, 5.74 and 5.47 ppm) of bridging HL^{2-}. This implies the presence of an intimate mixture of diastereomers of $\mathbf{2}^{2+}$ in the solution state which could not be separated even on preparative TLC plate.[14] Accordingly, calculated 74 aromatic proton resonances involving the two isomeric molecules (37 + 37) appear in the region δ, 8.8-5.0 ppm. The severe overlapping of

Dalton Transactions Accepted Manuscript

aromatic proton resonances due to their close chemical shift values in both **1** and $\mathbf{2}^{2+}$ has indeed prevented us to make the assignment for the individual signals.

Electronic structural aspects

The electronic structures in accessible redox states of mononuclear $\mathbf{1}^{n}$ (n=+1,0,-1,-2) and dinuclear $\mathbf{2}^{n}$ (n=+4,+3,+2,+1,0) have been evaluated *via* experimental investigation and DFT studies.

Mononuclear $\mathbf{1}^{n}$. The mononuclear complex **1** displays reversible one oxidation (Ox1) at 0.23 V and two successive reductions at -1.51 V (Red1) and -1.80 V (Red2) *versus* SCE (Fig. 2, Table 3). The HL^{2-} dominated HOMO of **1** (%HL^{2-}/Os: 88/8, Table 4 and Tables S3-S4†) and Mulliken spin density plot of $\mathbf{1}^{+}$ (HL^{2-}: 0.878 and Os: 0.220, Fig. 3 and Table 5) predict that HL^{2-} based orbitals are primarily involved in the oxidation process. However, appreciable spin density on the Os centre in $\mathbf{1}^{+}$ suggests a mixed electronic structural form of $[Os^{II}(bpy)_2(HL^{\bullet-})]^{+}$ (major)/$[Os^{III}(bpy)_2(HL^{2-})]^{+}$(minor) (Scheme 2). This has been further evidenced by the free radical type EPR spectrum of $\mathbf{1}^{+}$ with metal based partial anisotropic feature (g_1=2.127, g_2=2.096, g_3=2.046; <g>=2.089; Δg=0.08, Fig. 4).[19] On the other hand, ~ 90% bpy contributions in LUMO of **1**, SOMO of $\mathbf{1}^{-}$, α-LUMO of $\mathbf{1}^{-}$ (S=1/2) and SOMOs of $\mathbf{1}^{2-}$ (S=1, ΔE(S=0-S=1)=7050 cm^{-1}) (Table 4 and Tables S3, S5-S6†) as well as bpy centred spins in $\mathbf{1}^{-}$ (Mulliken spin density: 1.097(bpy)) and $\mathbf{1}^{2-}$ (Mulliken spin density: 1.620(bpy)) (Fig. 3, Table 5) support the exclusive involvement of bpy based orbitals in the stepwise reductions (Red1 and Red2 in Table 3) (Scheme 2).

Dalton Transactions Accepted Manuscript

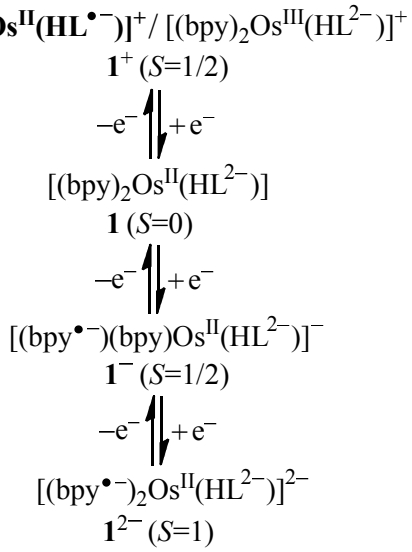

Scheme 2 Electronic structural forms of $\mathbf{1}^n$. Primary electronic structural form of $\mathbf{1}^+$ is shown in bold face.

The electronic transitions of $\mathbf{1}^n$ (n=0,+1) in CH_3CN are assigned based on TD-DFT calculations (Fig. 5, Table 6). In the visible region $Os^{II}(bpy)_2(HL^{2-})$ (**1**) exhibits one weak and broad transition centred at 720 nm (ε = 1740 $dm^3mol^{-1}cm^{-1}$) (TD-DFT: 653 nm) followed by one moderately intense transition at 518 nm (ε = 6680 $dm^3mol^{-1}cm^{-1}$) (TD-DFT: 496 nm) corresponding to bpy targeted interligand $(\pi)HL^{2-}\rightarrow(\pi^*)$bpy and $(d\pi)Os^{II}\rightarrow(\pi^*)$bpy MLCT (metal-to-ligand charge transfer) transitions, respectively. It also shows multiple intense interligand $(\pi)HL^{2-}\rightarrow(\pi^*)$bpy transitions in the higher energy UV region. On one-electron oxidation of coordinated HL^{2-} to $HL^{\bullet-}$ in $[Os^{II}(bpy)_2(HL^{\bullet-})]^+$ ($\mathbf{1}^+$), the low-energy interligand transition disappears and $(d\pi)Os^{II}\rightarrow(\pi^*)$bpy MLCT transition is appreciably blue shifted to 399 nm (ε = 6280 $dm^3mol^{-1}cm^{-1}$) (TD-DFT: 397 nm) with slight decrease in intensity. The oxidised

Dalton Transactions Accepted Manuscript

$\mathbf{1}^{+}$ also displays multiple intraligand ($(\pi)HL^{\bullet-}\rightarrow(\pi^*)HL^{\bullet-}$) and interligand ($(\pi)bpy\rightarrow(\pi^*)HL^{\bullet-}$) transitions in the UV region.

Dinuclear 2^{n}. The dinuclear complex $[(bpy)_2Os^{II}(\mu\text{-}H_2L^{2-})Os^{II}(bpy)_2]^{2+}$ ($\mathbf{2}^{2+}$) exhibits successive two oxidations at 0.24 V (Ox1) and 0.50 V (Ox2) and two reductions at -1.52 V (Red1) and -1.80 V (Red2) *versus* SCE (Fig. 2, Table 3). The first oxidation potential (Ox1) of the dinuclear complex $\mathbf{2}^{2+}$ is identical to that of the mononuclear complex **1** (Fig. 2, Table 3), implying the involvement of the relatively electron rich Os(1) centre (linked to the anionic carboxylate(O1) and imidazole(N1) donors, Scheme 1, Fig S3†) towards the initial oxidation process. The MO compositions of $\mathbf{2}^{2+}$ (S=0) (HOMO: Os/HL^{2-}: 65%/15%, Table 4 and Table S7†) and $\mathbf{2}^{3+}$ (S=1/2) (β-LUMO: $\%Os/HL^{2-}$: 72/11, Table 4 and Table S8†) as well as Mulliken spin density distribution in $\mathbf{2}^{3+}$ of Os1: 0.887, Os2: 0.005 and HL^{2-}: 0.117 (Fig. 3, Table 5) are collectively supportive of a mixed valent state of $[(bpy)_2Os^{III}(\mu\text{-}HL^{2-})Os^{II}(bpy)_2]^{3+}$ for $\mathbf{2}^{3+}$. However, the calculated reasonable spin accumulation of 0.117 on the bridge in $\mathbf{2}^{3+}$ reveals the minor contribution of the alternate electronic structural form i.e. radical ligand bridged isovalent metal ions $[(bpy)_2Os^{II}(\mu\text{-}HL^{\bullet-})Os^{II}(bpy)_2]^{3+}$.[9f-i,10d,20] It is therefore interesting to note that on insertion of the second metal fragment in the molecular framework of **1** the primary site of the oxidation process has been altered from HL^{2-} in **1** ($HL^{2-}\rightarrow HL^{\bullet-}$) to Os^{II} in $\mathbf{2}^{2+}$ ($Os^{II}\rightarrow Os^{III}$). Unfortunately, electrochemically generated mixed valent $\{Os^{III}(\mu\text{-}HL^{2-})Os^{II}\}$ state ($\mathbf{2}^{3+}$) fails to show any EPR even at 77 K as reported for other $Os^{III}Os^{II}$ mixed valent complexes.[6] The rapid relaxation process (time scale 10^{-8} s) due to close-lying excited states as well as relatively stronger spin-orbit coupling constant (λ,Os^{III}: 3000 cm^{-1}/Ru^{III}: 1000 cm^{-1} [12]) lead to EPR silent situation.[21] The MO compositions of β-HOMO of $\mathbf{2}^{3+}$ (S=1/2) ($\%Os/HL^{2-}$:71/15, Table 4 and Table S8†) and β-LUMO of $\mathbf{2}^{4+}$ (S=1, $\Delta E(S\text{=}0\text{-}S\text{=}1)$=7050 cm^{-1}) ($\%Os/HL^{2-}$:70/16, Table 4 and

Dalton Transactions Accepted Manuscript

Table S9†) in combination with Mulliken spin density distribution of Os1: 0.915, Os2: 0.811 and HL^{2-}: 0.275 (Fig.3, Table 5) in $\mathbf{2}^{4+}$ imply a metal based second oxidation process (Ox2) leading to the primary electronic configuration of $[(bpy)_2Os^{III}(\mu\text{-}HL^{2-})Os^{III}(bpy)_2]^{4+}$ for $\mathbf{2}^{4+}$ in conjunction with the minor involvement of the alternate electronic form of $[(bpy)_2Os^{III}(\mu\text{-}HL^{\bullet-})Os^{II}(bpy)_2]^{4+}$ (Scheme 3).[11h,22] The bpy dominated MOs (~90% bpy in LUMO of $\mathbf{2}^{2+}$, SOMO of $\mathbf{2}^{+}$, α-LUMO of $\mathbf{2}^{+}$ and SOMOs of **2,** Table 4 and Tables S7, S10-S11†) and Mulliken spin densities (1.1046/2.139(bpy) in $\mathbf{2}^{+}$/**2**, Fig. 3, Table 5) corroborate bpy based successive reduction processes (Red1 and Red2, Table 3, Scheme 3).

$$\mathbf{[(bpy)_2Os^{III}(\mu\text{-}HL^{2-})Os^{III}(bpy)_2]^{4+}}/\ [(bpy)_2Os^{III}(\mu\text{-}HL^{\bullet-})Os^{II}(bpy)_2]^{4+}$$
$$\mathbf{2}^{4+}\ (S=1)$$
$$-e^- \rightleftharpoons +e^-$$
$$\mathbf{[(bpy)_2Os^{III}(\mu\text{-}HL^{2-})Os^{II}(bpy)_2]^{3+}}/\ [(bpy)_2Os^{II}(\mu\text{-}HL^{\bullet-})Os^{II}(bpy)_2]^{3+}$$
$$\mathbf{2}^{3+}\ (S=1/2)$$
$$-e^- \rightleftharpoons +e^-$$
$$[(bpy)_2Os^{II}(\mu\text{-}HL^{2-})Os^{II}(bpy)_2]^{2+}$$
$$\mathbf{2}^{2+}\ (S=0)$$
$$-e^- \rightleftharpoons +e^-$$
$$[(bpy)(bpy^{\bullet-})Os^{II}(\mu\text{-}HL^{2-})Os^{II}(bpy)_2]^{+}$$
$$\mathbf{2}^{+}\ (S=1/2)$$
$$-e^- \rightleftharpoons +e^-$$
$$[(bpy)(bpy^{\bullet-})Os^{II}(\mu\text{-}HL^{2-})Os^{II}(bpy^{\bullet-})(bpy)]$$
$$\mathbf{2}\ (S=1)$$

Scheme 3 Electronic structural forms of $\mathbf{2}^{n}$. Primary electronic structural forms are shown in bold face.

Dalton Transactions Accepted Manuscript

The separation in potential between Ox1 and Ox2 of 0.26 V translates to the comproportionation constant (K_c) value of 8.2×10^4 ($RT\ln K_c = nF(\Delta E^0)$)[23] at the mixed valent $[(bpy)_2Os^{III}(\mu\text{-}HL^{2-})Os^{II}(bpy)_2]^{3+}$ ($\mathbf{2}^{3+}$) state. However, asymmetric coordination situation around the Os centres in $\mathbf{2}^{2+}$, carboxylate oxygen(O1), imidazole nitrogen(N1) *versus* imidazole nitrogen(N2), benzimidazole nitrogen(N3), implies that the separation in potential between Ox1 and Ox2 essentially originates due to the simultaneously operating dual effect of molecular asymmetry around the metal ions and the bridge (HL^{2-}) mediated intermetallic electrochemical coupling at the mixed valent $\{Os^{III}(\mu\text{-}HL^{2-})Os^{II}\}$ state.[11c,i] This indeed suggests that the bridge mediated intermetallic coupling driven K_c is much lower than that can simply be estimated *via* the separation in potential between the successive oxidation processes (Ox1/Ox2, Fig.2 and Table 3). Thus, the K_c value of lower than 10^4 represents a very weakly coupled class II or even a class I mixed valent situation according to Robin and Day classification[24] as has also been nicely reflected in the spin domination on one of the Os centres in $\mathbf{2}^{3+}$ (Fig. 3, Table 5).

$\mathbf{2}^{2+}$ displays two $(d\pi)Os^{II}\rightarrow(\pi^*)bpy$ MLCT transitions at 689 nm (ε = 5230 $dm^3mol^{-1}cm^{-1}$) (TD-DFT: 625 nm) and at 514 nm (ε = 18470 $dm^3mol^{-1}cm^{-1}$) (TD-DFT: 479 nm) due to the unsymmetrical feature of the bridge (HL^{2-}) (Fig. 5, Table 6). On one-electron oxidation to the mixed valent state in $[(bpy)_2Os^{III}(\mu\text{-}H_2L^{2-})Os^{II}(bpy)_2]^{3+}$ ($\mathbf{2}^{3+}$), the spectral profile changes slightly with the decrease in intensity. The visible bands at 621 nm (ε = 2990 $dm^3mol^{-1}cm^{-1}$) (TD-DFT: 593 nm), 504 nm (ε = 10170 $dm^3mol^{-1}cm^{-1}$) (TD-DFT: 482 nm) and 399 nm (ε = 14650 $dm^3mol^{-1}cm^{-1}$) (TD-DFT: 421 nm) are assigned based on the TD-DFT calculations as $(d\pi)Os/(\pi)HL^{2-}\rightarrow(\pi^*)bpy/(d\pi)Os\rightarrow(\pi^*)bpy$ MLLCT (metal/ligand-to-ligand charge transfer)/MLCT, $(d\pi)Os\rightarrow(\pi^*)bpy$ MLCT and $(\pi)bpy\rightarrow(d\pi)Os$ LMCT (ligand-to-metal charge

Dalton Transactions Accepted Manuscript

transfer) transitions, respectively. Though one weak Os(dπ)→Os(dπ) intervalence charge transfer (IVCT) transition has been predicted at 1360 nm for $\mathbf{2}^{3+}$ by TD-DFT calculations, no near-IR absorption is resolved experimentally. This implies the bridge mediated very weak to no intermetallic coupling at the mixed valent $\{Os^{III}(\mu\text{-}H_2L^{2-})Os^{II}\}$ state in $\mathbf{2}^{3+}$ as expected from a class I system.[9i,11b,25] The doubly oxidised isovalent higher congener $[(bpy)_2Os^{III}(\mu\text{-}H_2L^{2-})Os^{III}(bpy)_2]^{4+}$ ($\mathbf{2}^{4+}$) displays two weak LMCT transitions in the visible region at 507 nm (ε = 3120 $dm^3mol^{-1}cm^{-1}$) (TD-DFT: 539 nm) and 477 nm (ε = 3340 $dm^3mol^{-1}cm^{-1}$) (TD-DFT: 482 nm) corresponding to $(\pi)HL^{2-}\rightarrow(d\pi)Os$ and $(\pi)bpy\rightarrow(d\pi)Os$, respectively. The ligand based transitions: $(\pi)HL^{2-}\rightarrow(\pi^*)bpy$, $bpy(\pi)\rightarrow HL^{2-}(\pi^*)$ and $bpy(\pi)\rightarrow bpy(\pi^*)$ appear in the higher energy UV-region in each redox state.

Selective anion sensing features of 1 and $\mathbf{2}^{2+}$

The potential application of mononuclear (**1**) and dinuclear ($[\mathbf{2}](ClO_4)_2$) osmium complexes encompassing one N-H group in the framework of coordinated HL^{2-} towards the recognition of selective anion(s) has been evaluated *via* different experimental and DFT calculations.

The initial assessment of anion sensing event has been made by monitoring the colour change of the acetonitrile solution of **1** or $\mathbf{2}^{2+}$ on addition of anions such as F^-, Cl^-, Br^-, I^-, OAc^-, SCN^-, HSO_4^- and $H_2PO_4^-$. Though distinct colour change of **1** or $\mathbf{2}^{2+}$ (brown to pink) has been noticed on addition of one equivalent of F^- ion, no change in colour occurs with the introduction of other aforesaid anions even up to 8 equivalents (Fig. 6 and Fig. S4†). This implies that both **1** and $\mathbf{2}^{2+}$ function as effective colorimetric receptors selectively for the F^- ion.

The selective recognition of F^- ion by **1** or $\mathbf{2}^{2+}$ has been corroborated *via* spectrophotometric titrations in the presence of the aforesaid anions. The UV-vis. spectrum of **1** or $\mathbf{2}^{2+}$ in acetonitrile

Dalton Transactions Accepted Manuscript

remains unaltered on addition of up to 8 equivalent TBA (tetrabutylammonium) salt of Cl^- or Br^- or I^- or OAc^- or SCN^- or HSO_4^- or $H_2PO_4^-$. However, MLCT bands of **1** and $\mathbf{2}^{2+}$ at 518 nm and 514 nm, respectively, are appreciably red-shifted to 545 nm in the presence of one equivalent of F^- (Fig. 7 and Fig. S5†), implying a F^- selective process. The second-sphere donor-acceptor interaction between the metal coordinated HL^{2-} and the F^- ion enhances electron density on the metal ion which in turn pushes the MLCT band to the lower energy region.[26] The spectrophotometric titration of **1** or $\mathbf{2}^{2+}$ with the F^- ion passes through two clear isosbestic points at 338 nm, 530 nm or 328 nm, 530 nm, respectively (Fig. 8 and Fig. S6†). The observed spectral saturation by one equivalent F^- (inset of Fig. 8 and Fig. S6†) suggests a 1:1 receptor-anion interaction. The binding constant (K) of **1** or $\mathbf{2}^{2+}$ with the F^- ion has been calculated based on eqns (1) and (2),[27] where ΔA represents the change in initial absorbance at 518 or 514 nm for **1** or $\mathbf{2}^{2+}$, respectively, upon each addition of F^-. $[M(HL)]^{n+}$ and

$$[\{M(HL)\}]^{n+} + F^- \longrightarrow [\{M(HL)\}]^{n+} \cdot F^-] \longrightarrow [\{M(HL)\}]^{(n-1)} + HF \quad (1)$$

$$K = \frac{[M(HL)^{n+} \cdot F^-]}{[M(HL)^{n+}][F^-]}$$

$$\Delta A = \frac{\Delta\varepsilon\,([M(HL)^{n+}] + F^-] + 1/K) + (\Delta\varepsilon^2\,([M(HL)^{n+}] + [F^-] + 1/K)^2 - 4\Delta\varepsilon^2\,[M(HL)^{n+}][F^-])^{1/2}}{2} \quad (2)$$

$[F^-]$ correspond to the concentration of the respective receptors **1**, $\mathbf{2}^{2+}$ and anion during the spectrophotometric titrations. The binding constant (K) and the change in molar extinction coefficient ($\Delta\varepsilon$) are calculated by the nonlinear curve fitting procedure using ΔA at each concentration of F^- which result in log K = 6.83 and 5.89 for **1** and $\mathbf{2}^{2+}$, respectively (Fig. S7†).

Dalton Transactions Accepted Manuscript

The spectrophotometric titrations of **1** and $\mathbf{2}^{2+}$ with one-equivalent strong base, TBAOH have been carried out (Fig. S8†) and changes in spectral patterns bear a resemblance to that obtained with TBAF (Fig. 8 and Fig. S6†). This indeed suggests a hydrogen bonding interaction between the pendant NH proton of **1** or $\mathbf{2}^{2+}$ and the anion, followed by proton abstraction.[28] The pK_a values of **1** and $\mathbf{2}^{2+}$ of 9.8 and 8.5, respectively, are estimated by monitoring the pH dependent spectral changes in 1:1 CH_3CN-H_2O. The selective F^- sensing feature of **1** or $\mathbf{2}^{2+}$ could be qualitatively correlated to the basicity (pK_a(aq)) of the halogen acids: HF (3.45) > HCl (-7) > HBr (-9) > HI (-11) and the oxy-anions: HOAc (4.75) > H_3PO_4 (2.12) > H_2SO_4 (-2) > HSCN (~ -2).[29] The inability of **1** or $\mathbf{2}^{2+}$ to recognise OAc^- in spite of its relatively higher pK_a(aq) value suggests that the collective impact of the basicity of anion and the strength of the hydrogen bonding interaction influences the eventual transfer of the N-H proton from the receptor to the anion.

The anion recognition features of **1** and $\mathbf{2}^{2+}$ have also been evaluated by following the change in redox potential(s) of the oxidation processes (Ox1, Ox2 in Fig. 2) as a function of addition of different anions using cyclic and differential pulse voltammetric techniques. The gradual additions of TBA salt of F^- up to one equivalent to the acetonitrile solution of **1** result in a negative shift of the initial oxidation potential, E^0/V at 0.23 V to 0.08 V (Fig. 9) and no further change in E^0 value has been observed on further addition of F^- up to 8 equivalents. However, no identifiable shift in E^0 value occurs on addition of other anions (up to 8 equivalents of Cl^-, Br^-, I^-, OAc^-, SCN^-, HSO_4^- and $H_2PO_4^-$) in the solution of **1**. Similarly, E^0 values (Ox1 and Ox2, Fig. 2) of the dinuclear complex $\mathbf{2}^{2+}$ at 0.24 V and 0.5 V (K_c: 2.5x10^4) shift to 0.1 V and 0.22 V (K_c: 1.08x10^2) with the lowering in K_c value only on selective addition of one equivalent of F^- (Fig. 9). Thus, in accordance with the colorimetric as well as spectrophotometric observations

Dalton Transactions Accepted Manuscript

(see above), mononuclear **1** and the corresponding dinuclear $\mathbf{2}^{2+}$ can also function as excellent electrochemical receptors for the selective recognition of F^-. The deprotonation of the free benzimidazole NH proton in the framework of **1** or $\mathbf{2}^{2+}$ by the influence of F^- ion increases the residual electron density on the metal centre which in turn decreases the oxidation potentials. This has been further recognised *via* the similar shift in voltammetric responses on addition of one equivalent of TBAOH to the CH_3CN solution of **1** or $\mathbf{2}^{2+}$.

The effective interaction of **1** or $\mathbf{2}^{2+}$ with the F^- ion has also been probed by ^{1}H-NMR titrations in $CDCl_3$. On sequential additions of TBAF up to one equivalent to the solution of **1**, the free N-H proton associated with the coordinated HL^{2-} at δ, 13.93 ppm initially shifts to the downfield region and finally disappears due to its eventual abstraction by the F^- ion as HF (Fig. 10). The effect of removal of the N-H proton of **1** by F^- has also been reflected in the slight upfield shift of the imidazole ring C-H singlet at δ, 6.6 ppm to 6.5 ppm as well as slight change in chemical shifts of the other aromatic protons. Similar to **1**, the free benzimidazole N-H protons of HL^{2-} for the diastereomeric mixture (1:1 ratio) of $\mathbf{2}^{2+}$ in $CDCl_3$ at δ, 11.78 ppm and 11.65 ppm disappear on addition of one equivalent of TBAF (Fig. S9†). However, on addition of TBAF, two CH protons associated with the imidazole ring of HL^{2-} in diastereomeric $\mathbf{2}^{2+}$ behave differently, one CH proton expectedly moves slightly to the upfield region (δ, 5.47 ppm→5.42 ppm) as in the case of **1** while the other CH proton moves in the opposite direction (δ, 5.74 ppm→5.8 ppm), possibly due to its weak hydrogen bonding interaction with the fluoride ion present in the solution.[15l,30] No noticeable change in the ^{1}H-NMR spectral profiles of both **1** and $\mathbf{2}^{2+}$ has been occurred either on addition of more than one equivalent of F^- ion or in the presence of other anions (Cl^-, Br^-, I^-, OAc^-, SCN^-, $HSO4^-$ and $H_2PO_4^-$ even up to 8 equivalents).

Dalton Transactions Accepted Manuscript

The ^{19}F-NMR of TBAF in $CDCl_3$ displays one sharp signal at -81.02 ppm and one more signal at -122.3 ppm corresponding to TBAF and HF_2^-, respectively, (Fig. S10†) where HF_2^- signal develops due to the presence of moisture in the system. However, addition of TBAF to the 0.6 equivalent of **1** or $\mathbf{2}^{2+}$ leads to the disappearance of the TBAF signal at -81.02 ppm with the concomitant intensity enhancement of the HF_2^- signal at -122.3 ppm. This possibly justifies the initial N-H···F hydrogen bonding interaction between **1** or $\mathbf{2}^{2+}$ and TBAF followed by proton abstraction to result in HF which further reacts with the excess F^- present in the system to give HF_2^-.[27a, b, 31]

The hydrogen bond-mediated anion sensing process has been rationalised on the basis of NBO calculations. The appreciably longer N4-H4 distance of 1.320 Å in optimised **A** as compared to that in optimised **1** (1.028 Å) as well as H4-F distance of 1.118 Å, N4-H4···F angle of 174.1° in **A** collectively suggest a hydrogen bonded anion sensing mechanism (Scheme 4). The decrease in natural charge on N4 (-0.602) and the simultaneous increase in natural charge on H4 (0.518) in optimised **A** with regard to optimised **1** (N4: -0.570 and H4: 0.458) (Table S12†) also support the hydrogen bonded anion sensing mechanism.[13,32]

Similarly, the N4-H4 bond distance in optimised **B** increases to 1.763 Å from 1.028 Å in optimised $\mathbf{2}^{2+}$ (Scheme 4). This in conjunction with the calculated H4-F distance (0.96 Å) and N4-H4···F angle (149.6°) in **B** as well as the decrease and increase of the natural charges on N4 (-0.542) and H4 (0.563), respectively, with respect to that of $\mathbf{2}^{2+}$ (N4: -0.530 and H4: 0.484) (Table S12†) imply the hydrogen bonded anion sensing mechanism.

Dalton Transactions Accepted Manuscript

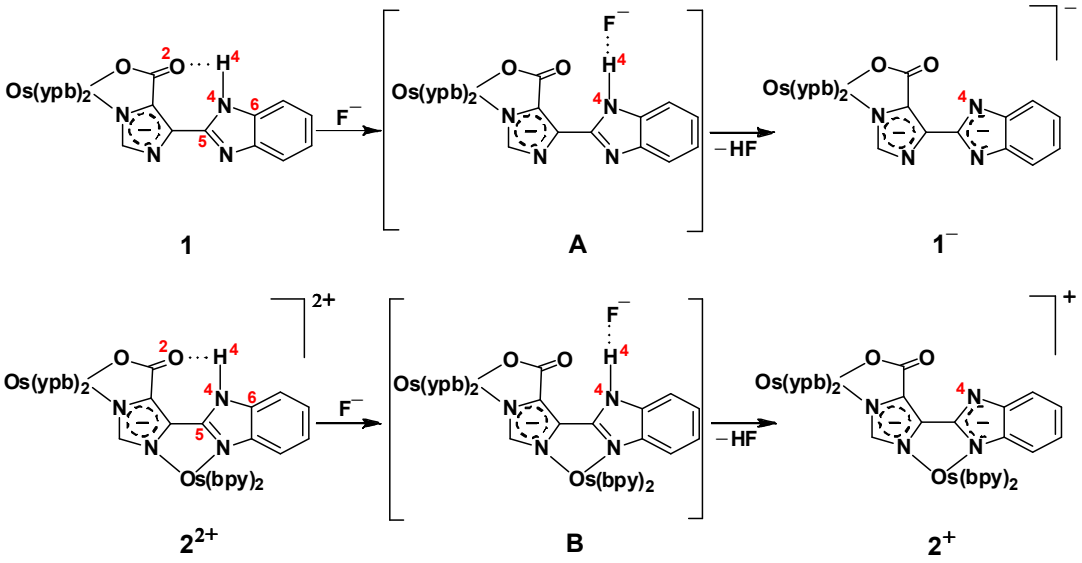

Scheme 4 Transformations of **1**→**1**$^{-}$ and **2**$^{2+}$→**2**$^{+}$ in presence of F^{-}.

The formation of intermediate **A** or **B** *via* the interaction of **1** or **2**$^{2+}$, respectively, with TBAF in CH_3CN has also been evidenced by *in situ* generated mass data, which exhibit peaks at *m/z* = 751.08 and 1349.72 corresponding to [**1**+2H+F^{-}] (**A** in Scheme 4, calculated mass: 751.16), and [**2**$^{2+}$+F^{-}] (**B** in Scheme 4, calculated mass, 1349.79), respectively (Fig. S11†).

Conclusions

The experimental and theoretical (DFT) investigations collectively reveal the redox non-innocent potential of the partially deprotonated HL^{2-} (H_3L=5-(1*H*-benzo[*d*]imidazol-2-yl)-1*H*-imidazole-4-carboxylic acid) in the newly designed mononuclear $[Os^{II}(bpy)_2(HL^{2-})]^n$ (**1**^{n}) and asymmetric dinuclear $[(bpy)_2Os^{II}(\mu\text{-}HL^{2-})Os^{II}(bpy)_2]^n$ (**2**^{n}) complexes, leading to mixed electronic structural forms at the oxidised states (Schemes 2 and 3). The electrochemically generated unsymmetrical ligand (HL^{2-}) bridged mixed valent $\{Os^{III}(\mu\text{-}HL^{2-})Os^{II}\}$ state in **2**$^{3+}$ fails to show the expected EPR at 77 K due to rapid relaxation process as well as IVCT transition up to 2000 nm owing to bridge mediated very weak to no intermetallic electronic coupling (class I). Further, both **1** and

Dalton Transactions Accepted Manuscript

$\mathbf{2}^{2+}$ encompassing one N-H proton associated with the coordinated HL^{2-} ligand are established to be equally efficient in recognising F^- ion selectively (log *K*: 6.83 (**1**) and 5.89 ($\mathbf{2}^{2+}$)) over the other tested anions, Cl^-, Br^-, I^-, OAc^-, SCN^-, HSO_4^- and $H_2PO_4^-$.

Dalton Transactions Accepted Manuscript

Experimental section

Materials

The starting complexes *cis*-[Os(bpy)$_2$Cl$_2$][33] and the ligand 5-(1*H*-benzo[*d*]imidazol-2-yl)-1*H*-imidazole-4-carboxylic acid (H_3L)[13] were prepared as per the reported procedures. Tetrabutylammonium (TBA) salts of F^-, Cl^-, Br^-, I^-, HSO_4^-, OAc^-, $H_2PO_4^-$, SCN^-, OH^- were obtained from Aldrich or Alfa Aesar. Imidazole-4,5-dicarboxylic acid and 1,2-phenylenediamine were purchased from Merck, India. Other chemicals and solvents were reagent grade and used as received. For spectroscopic and electrochemical studies HPLC grade solvents were used.

Physical measurements

UV-vis-NIR studies were performed on a Perkin-Elmer Lambda 950 spectrophotometer. FT-IR spectra were taken on a Nicolet spectrophotometer with samples prepared as KBr pellets. Cyclic voltammetry, differential pulse voltammetry and coulometric measurements were carried out using a PAR model 273A electrochemistry system. Glassy carbon working electrode, Pt auxiliary electrode and an aqueous saturated calomel reference electrode (SCE) were used in a three-electrode configuration. The supporting electrolyte was 0.1 mol dm^{-3} [Et_4N][ClO_4] and the solute concentration was ~ 10^{-3} mol dm^{-3}. The half-wave potential E^o_{298} was set equal to 0.5(E_{pa} + E_{pc}), where E_{pa} and E_{pc} are anodic and cathodic cyclic voltammetric peak potentials, respectively. A platinum wire-gauze working electrode was used in the coulometric experiments. All electrochemical experiments were carried out under dinitrogen atmosphere. ^{1}H-NMR and ^{19}F-NMR spectra were recorded using a Bruker Avance III 500 MHz spectrometer. Trifluoro-toluene was used as an internal standard in $CDCl_3$ for recording ^{19}F- NMR spectra. The electrical conductivity of the solution was checked by using an Autoranging conductivity meter (Toshcon Industries, India). The elemental analyses were carried out on a Thermoquest (EA 1112) micro

Dalton Transactions Accepted Manuscript

analyser. Electrospray mass spectra were recorded on a Bruker's Maxis Impact (282001.00081). For spectrophotometric titrations, in each step 2 μL aliquot of the TBA salt of the respective anions ($5x10^{-3}$ mol dm^{-3}) in CH_3CN was added by a micro-syringe in 2 cm^3 CH_3CN solution of of **1** or $\mathbf{2}^{2+}$ ($5x10^{-5}$ mol dm^{-3}) using a quartz cuvette with 1 cm path length. For electrochemical titration, 40 μL aliquot of the TBA salt of the respective anions ($5x10^{-2}$ mol dm^{-3}) in acetonitrile was added by a micropipette in each step in 10 cm^3 acetonitrile solution of (10^{-3} mol dm^{-3}) of **1** or $\mathbf{2}^{2+}$.

Cerium ammonium nitrate (CAN) titrations

The acetonitrile solution of CAN ($1x10^{-3}$ mol dm^{-3}) was gradually added to the acetonitrile solution of **1** or $\mathbf{2}^{2+}$ ($1x10^{-4}$ mol dm^{-3}) up to 1 or 2 equivalent, respectively, in a cuvette with 1 cm light path length. The absorption spectral changes were monitored after each addition. Each absorption spectrum was plotted on appropriate consideration of the volume change on addition of CAN solution.

Crystallography

Single crystals of **1** and [**2**]$(Cl)_2$ were grown by slow evaporation of their acetonitrile-methanol(1:1) and chloroform solutions, respectively. X-ray diffraction data of **1** and [**2**]$(Cl)_2$ were collected using OXFORD XCALIBUR CCD and RIGAKU/SATURN-724 CCD single crystal X-ray diffractometers, respectively. The structures were solved and refined by full-matrix least-squares techniques on F^2 using the SHELX-97 program.[34] All data were corrected for Lorentz polarisation and absorption effects. The absorption corrections for **1** and [**2**]$(Cl)_2$ were performed by multi-scan technique and numerical method. Hydrogen atoms were included in the refinement using the riding model. The non-hydrogen atoms were refined anisotropically. **1** and

Dalton Transactions Accepted Manuscript

[**2**](Cl)$_2$ were crystallised with 3 molecules of water and chloroform, respectively. Hydrogen atoms associated with the chloform molecules of [**2**](Cl)$_2$ could not be located due to bad data quality, however, their contributions have been considered for molecular composition in Table S1†.

Computational details

Full geometry optimisations were carried out at the (R)B3LYP (for **1**, $\mathbf{2}^{2+}$, **A** and **B**) and at the (U)B3LYP levels (for $\mathbf{1}^{+}$, $\mathbf{1}^{-}$, $\mathbf{1}^{2-}$, **2**, $\mathbf{2}^{+}$, $\mathbf{2}^{3+}$ and $\mathbf{2}^{4+}$), using density functional theory method with Gaussian 09 program package.[35] All elements except osmium were assigned the 6-31G(d) basis set. The LANL2DZ basis set with effective core potential was employed for the osmium atom.[36] The vibrational frequency calculations were performed to ensure that the optimised geometries represent the local minima and there are only positive eigen values. Vertical electronic excitations based on (R)B3LYP/(U)B3LYP optimised geometries were computed for $\mathbf{1}^{n}$ (n= +1, 0) and $\mathbf{2}^{n}$ (n = +4, +3, +2,) using the time-dependent density functional theory (TD-DFT) formalism[37] in acetonitrile using conductor-like polarisable continuum model (CPCM).[38] Natural bond orbital analysis was performed using the NBO 3.1 module of Gaussian 09 on optimised geometries. *Chemissian 1.7*[39] was used to calculate the fractional contributions of various groups to each molecular orbital. All calculated structures were visualized with *ChemCraft*.[40]

Preparation of Complexes

Synthesis of [(bpy)$_2$Os^{II}(HL^{2-})] (1). A mixture of the precursor complex *cis*-[Os(bpy)$_2$Cl$_2$] (100 mg, 0.17 mmol), the preformed ligand H_3L (46 mg, 0.20 mmol) and the base NEt_3 (19 mg, 0.20 mmol) in 30 cm^3 ethanol-water (2:1) mixture was heated at reflux for 60 h under dinitrogen atmosphere with simultaneous mechanical stirring. The initial red colour changed to deep brown. The solvent of the reaction mixture was evaporated to dryness under reduced pressure. It was

Dalton Transactions Accepted Manuscript

then purified using a neutral alumina column. The reddish band corresponding to **1** was eluted by CH_3CN-CH_3OH (1:1). The pure complex **1** was obtained in the solid form on removal of solvent under reduced pressure. Yield: 64 mg, 50%. Anal. calcd for $OsC_{31}H_{22}N_8O_2$: C 51.09, H 3.04, N 15.38; Found: C, 50.39; H, 3.33; N, 15.65. ESI-MS(+) in CH_3CN, *m/z*: calcd for $\{\mathbf{1} + H\}^+$:731.14. Found: 731.17.^{1}H NMR (500 MHz, $CDCl_3$): δ, (ppm, *J*(Hz)): 13.93(s, 1H, N4H4), 8.99(d, 1H, 6), 8.13(d, 2H, 8), 8.02(t, 2H, 8), 7.98(d, 1H, 6), 7.72(d, 2H, 6), 7.33(m, 6H), 7.43(m, 4H), 6.86(t, 1H, 6), 6.76(t, 1H, 7), 6.60(s, 1H, imidazole C-H).

Synthesis of $[(bpy)_2Os^{II}(\mu\text{-}HL^{2-})Os^{II}(bpy)_2](Cl)_2$ ([2](Cl)$_2$)/$[(bpy)_2Os^{II}(\mu\text{-}HL^{2-})Os^{II}(bpy)_2](ClO_4)_2$ ([2](ClO$_4$)$_2$).

[2](Cl)$_2$. The mononuclear complex $[(bpy)_2Os(HL^{2-})]$ (**1**) (120 mg, 0.17 mmol) and the precursor *cis*-$[Os(bpy)_2Cl_2]$ (100 mg, 0.17 mmol) were taken in 30 cm^3 ethanol:water (2:1) mixture. The resultant mixture was heated at reflux for 48 h under dinitrogen atmosphere with simultaneous mechanical stirring. The solution was then evaporated under reduced pressure. The solid mass thus obtained was purified by using a neutral alumina column. The pure [**2**](Cl)$_2$ was eluted by 3:1 CH_3CN-CH_3OH. Yield: 80 mg, 45%. Anal. calcd for $Os_2C_{51}H_{38}N_{12}O_2Cl_2$: C 47.04, H 2.94, N 12.91; Found: C, 46.97; H, 2.99; N, 13.01. Λ_M (Ω^{-1} cm^2 M^{-1}) in acetonitrile at 298 K: 185. ESI-MS(+) in CH_3CN, *m/z*: calcd for $\{[\mathbf{2}]Cl\}^+$: 1266.79, Found: 1266.89.

[2](ClO$_4$)$_2$. The initial reaction solution as stated above was concentrated to 5 cm^3 on a rotary evaporator and an aqueous saturated $NaClO_4 \cdot H_2O$ solution was added to it. The brown precipitate thus obtained was filtered and washed thoroughly with ice-cold water followed by cold ethanol. The dried solid mass was purified using a neutral alumina column. The dark brown band corresponding to complex [**2**](ClO$_4$)$_2$ was eluted by CH_3CN-CH_3OH (2:1). The solid pure

Dalton Transactions Accepted Manuscript

complex [**2**]$(ClO_4)_2$ was obtained on removal of solvent under reduced pressure. Yield: 94 mg, 48%. Anal. calcd for $Os_2C_{51}H_{38}N_{12}O_{10}Cl_2$: C 42.83, H 2.68, N 11.75; Found: C, 42.63; H, 2.77; N, 11.62. Λ_M (Ω^{-1} cm^2 M^{-1}) in acetonitrile at 298 K: 190. ESI-MS(+) in CH_3CN, *m/z*: calcd for $\{[\mathbf{2}]ClO_4\}^+$: 1330.79, Found: 1330.72.

(*CAUTION*! Perchlorate salts are potentially explosive and should be handled with appropriate care).

Acknowledgements

Financial support received from the Department of Science and Technology, Council of Scientific and Industrial Research (Fellowship to AD, HA, PG), New Delhi, India is gratefully acknowledged. Special acknowledgment is made to the Sophisticated Analytical Instrument Facility (SAIF), Indian Institute of Technology, Bombay, for providing the EPR facility.

Dalton Transactions Accepted Manuscript

References

1 (*a*) C. Creutz and H. Taube, *J. Am. Chem. Soc.*, 1969, **91**, 3988; (*b*) C. Creutz and H. Taube, *J. Am. Chem. Soc.*, 1973, **95**, 1086.

2 (*a*) D. P. Rillema and K. B. Mack, *Inorg. Chem.*, 1982, **21**, 3849; (*b*) C. H. Braunstein, A. D. Baker, T. C. Strekas and H. D. Gafney, *Inorg. Chem.*, 1984, **23**, 857; (*c*) R. R. Ruminski, T. Cockroft and M. Shoup, *Inorg. Chem.*, 1988, **27**, 4026; (*d*) V. Balzani, A. Juris, M. Venturi, S. Campagna and S. Serroni, *Chem. Rev.*, 1996, **96**, 759; (*e*) A. Gourdon and J.-P. Launay, *Inorg. Chem.* 1998, **37**, 5336; (*f*) P. Bonhôte, A. Lecas and E. Amouyal, *Chem. Commun.*, 1998, 885; (*g*) G. Denti, S. Campagna, L. Sabatino, S. Serroni, M. Ciano and V. Balzani, *Inorg. Chem.*, 1990, **29**, 4750; (*h*) A. M. Stadler, F. Puntoriero, S. Campagna, N. Kyritsakas, R. Welter and J. M. Lehn, *Chem.–Eur. J.*, 2005, **11**, 3997; (*i*) W. R. Browne, N. M. O'Boyle, W. Henry, A. L. Guckian, S. Horn, T. Fett, C. M. O'Connor, M. Duati, L. De Cola, C. G. Coates, K. L. Ronayne, J. J. McGarvey and J. G. Vos, *J. Am. Chem. Soc.*, 2005, **127**, 1229; (*j*) D. M. D'Alessandro, A. C. Topley, M. S. Davies and F. R. Keene, *Chem.–Eur. J.*, 2006, **12**, 4873; (*k*) D. M. D'Alessandro and F. R. Keene, *New J. Chem.*, 2006, **30**, 228; (*l*) S. Maji, B. Sarkar, S. M. Mobin, J. Fiedler, W. Kaim and G. K. Lahiri, *Dalton Trans.*, 2007, 2411; (*m*) F. Loiseau, F. Nastasi, A. M. Stadler, S. Campagna and J. M. Lehn, *Angew. Chem. Int. Ed.*, 2007, **46**, 6144; (*n*) S. Stagni, E. Orselli, A. Palazzi, L. De Cola, S. Zacchini, C. Femoni, M. Marcaccio, F. Paolucci and S. Zanarini, *Inorg. Chem.*, 2007, **46**, 9126; (*o*) P. Govindaswamy, B. Therrien, G. Süss-Fink, P. Štěpnička and J. Ludvík, *J. Organomet. Chem.*, 2007, **692**, 1661; (*p*) S. Ghumaan, B. Sarkar, M. P. Patil, J. Fiedler, R. B. Sunoj, W. Kaim and G. K. Lahiri, *Polyhedron*, 2007, **26**, 3409; (*q*) B. Therrien, G. Süss-Fink, P. Govindaswamy and

Dalton Transactions Accepted Manuscript

C. Saïd-Mohamed, *Polyhedron*, 2007, **26**, 4065; (*r*) J.-M. Herrera, S. J. A. Pope, A. J. H. M. Meijer, T. L. Easun, H. Adams, W. Z. Alsindi, X.-Z. Sun, M. W. George, S. Faulkner and M. D. Ward, *J. Am. Chem. Soc.*, 2007, **129**, 11491; (*s*) S. Xun, J. Zhang, X. Li, D. Ma and Z. Y. Wang, *Synth. Met.*, 2008, **158**, 484; (*t*) J. C. Salsman, C. P. Kubiak and T. Ito, *J. Am. Chem. Soc.*, 2005, **127**, 2382; (*u*) C. H. Londergan, J. C. Salsman, B. J. Lear and C. P. Kubiak, *Chem. Phys.*, 2006, **57**, 324.

3 (*a*) N. S. Hush, *Prog. Inorg. Chem.*, 1967, **8**, 391; (*b*) N. S. Hush, *Coord. Chem. Rev.*, 1985, **64**, 135; (*c*) C. Creutz, M. D. Newton and N. Sutin, *J. Photochem. Photobiol. A*, 1994, **82**, 47.

4 (*a*) V. Petrov, J. T. Hupp, C. Mottley and L. C. Mann, *J. Am. Chem. Soc.*, 1994, **116**, 2171; (*b*) D. H. Oh, M. Sano and S. G. Boxer, *J. Am. Chem. Soc.*, 1991, **113**, 6880; (*c*) R. C. Rocha, M. G. Brown, C. H. Londergan, J. C. Salsman, C. P. Kubiak and A. P. Shreve, *J. Phys. Chem. A*, 2005, **109**, 9006.

5 (*a*) K, Prassides, Ed. *Mixed Valency Systems - Applications in Chemistry, Physics and Biology*; Kluwer Academic Publishers: Dordrecht, 1991; (*b*) M. Fabre and J. Bonvoisin, *J. Am. Chem. Soc.*, 2007, **129**, 1434; (*c*) D. E. Richardson and H. Taube, *Coord. Chem. Rev.*, 1984, **60**, 107; (*d*) R. J. Crutchley, *Adv. Inorg. Chem.*, 1994, **41**, 273; (*e*) K. D. Demadis, D. C. Hartshorn and T. J. Meyer, *Chem. Rev.*, 2001, **101**, 2655; (*f*) B. S. Brunschwig, C. Creutz, N. Sutin, *Chem. Soc. Rev.*, 2002, **31**, 168; (*g*) J.-P. Launay, *Chem. Soc. Rev.*, 2001, **30**, 386; (*h*) M. D. Ward, *Chem. Soc. Rev.*, 1995, **24**, 121; (*i*) J. A. McCleverty, M. D. Ward, *Acc. Chem. Res.,* 1998, **31**, 842; (*j*) D. Astruc, *Acc. Chem. Res.*, 1997, **30**, 383; (*k*) D. M. D'Alessandro, F. R. Keene, *Chem. Soc. Rev.*, 2006, **35**, 424; (*l*) J. T. Hupp, *Comprehensive Coordination Chemistry II*, Ed. J. A. McCleverty, T.

Dalton Transactions Accepted Manuscript

J. Meyer, Elsevier Science: Amsterdam, 2003, p.709; (*m*) R. J. Crutchley, *Comprehensive Coordination Chemistry II,* Ed. J. A. McCleverty, T. J. Meyer, Elsevier Science: Amsterdam, 2003, p. 235; (*n*) W. Kaim and B. Sarkar, *Coord. Chem. Rev.*, 2007, **251**, 584.

6 (*a*) T. Scheiring, W. Kaim, J. A. Olabe, A. R. Parise and J. Fiedler, *Inorg. Chim. Acta*, 2000, **125**, 300; (*b*) W. Kaim and B. Sarkar, *Coord. Chem. Rev.*, 2013, **257**, 1650; (*c*) J. J. Concepcion, D.M. Dattelbaum, T.J. Meyer and R.C. Rocha, *Philos. Trans. R. Soc. A*, 2008, **366**, 163; (*d*) W. Kaim and G. K. Lahiri, *Angew. Chem. Int. Ed.*, 2007, **46**, 1778.

7 (*a*) S. B. Braun-Sand and O. Wiest, *J. Phys. Chem. B*, 2003, **107**, 9624; (*b*) S. B. Braun-Sand and O. Wiest, *J. Phys. Chem. B*, 2003, **107**, 285; (*c*) Y. Wang and M. Lieberman, *IEEE Trans. Nanotech.*, 2004, **3**, 368; (*d*) P. Zhao, D. Woolard, J. M. Seminario and R. Trew, *Int. J. High Speed Electronics*, 2006, **16**, 705; (*e*) C. S. Lent, B. Isaksen, M. Lieberman, *J. Am. Chem. Soc.*, 2003, **125**, 1056.

8 (*a*) J. A. Baumann and T. J. Meyer, *Inorg. Chem.*, 1980, **19**, 345; (*b*) A. F. Heyduk, D. G. Nocera, *Science*, 2001, **293***,* 1639.

9 (*a*) R. Ruminski, J. Kiplinger, T. Cockroft and C. Chase, *Inorg. Chem.*, 1989, **28**, 370; (*b*) C. R. Arana and H. D. Abruña, *Inorg. Chem.*, 1993, **32**, 194; (*c*) D. M. Dattelbaum, C. M. Hartshorn and T. J. Meyer, *J. Am. Chem. Soc.*, 2002, **124**, 4938; (*d*) C. M. Hartshorn, N. Daire, V. Tondreau, B. Loeb, T. J. Meyer and P. S. White, *Inorg. Chem.*, 1999, **38***,* 3200; (*e*) N. Chanda, R. H. Laye, S. Chakraborty, R. L. Paul, J. C. Jeffery, M. D. Ward and G. K. Lahiri, *J. Chem. Soc.*, *Dalton Trans.*, 2002, 3496; (*f*) N. Chanda, B. Sarkar, J. Fiedler, W. Kaim and G. K. Lahiri, *Dalton Trans*., 2003, 3550; (*g*) N. Chanda, B. Sarkar, S. Kar, J. Fiedler, W. Kaim and G. K. Lahiri, *Inorg. Chem*., 2004, **43**, 5128; (*h*) S. Ghumaan, B.

Dalton Transactions Accepted Manuscript

Sarkar, N. Chanda, M. Sieger, J. Fiedler, W. Kaim and G. K. Lahiri, *Inorg. Chem.*, 2006, **45**, 7955; (*i*) M. Koley, B. Sarkar, S. Ghumaan, E. Bulak, J. Fiedler, W. Kaim and G. K. Lahiri, *Inorg. Chem.*, 2007, **46**, 3736; (*j*) S. H. Wadman, R. W. A. Havenith, F. Hartl, M. Lutz, A. L. Spek, G. P. M. van Klink and G. van Koten, *Inorg. Chem.*, 2009, **48**, 5685; (*k*) T. Kundu, B. Sarkar, T. K. Mondal, J. Fiedler, S. M. Mobin, W. Kaim and G. K. Lahiri, *Inorg. Chem.*, 2010, **49**, 6565; (*l*) T. Kundu, B. Sarkar, T. K. Mondal, S. M. Mobin, F. A. Urbanos, R. Jiménez-Aparicio, J. Fiedler, W. Kaim and G. K. Lahiri, *Inorg. Chem.*, 2011, **50**, 4753; (*m*) R. C. Rocha, F. N. Rein, H. Jude, A. P. Shreve, J. J. Concepcion and T. J. Meyer, *Angew. Chem. Int. Ed.*, 2008, **47**, 503; (*n*) A. K. Das, B. Sarkar, J. Fiedler, S. Záliš, I. Hartenbach, S. Strobel, G. K. Lahiri and W. Kaim, *J. Am. Chem. Soc.*, 2009, **131**, 8895; (*o*) S. Bernhard, K. Takada, D. J. Díaz, H. Abruña and H. Mürne, *J. Am. Chem. Soc.*, 2001, **123**, 10265; (*p*) S. Fantacci, F. D. Angelis, J. Wang, S. Bernhard and A. Selloni, *J. Am. Chem. Soc.*, 2004, **126**, 9715; (*q*) L. M. Vogler and K. J. Brewer, *Inorg. Chem.*, 1996, **35**, 818; (*r*) S. W. Jones, L. M. Vrana and K. J. Brewer, *J. Organomet. Chem.*, 1998, **554**, 29; (*s*) W. Chen, F. N. Rein, B. L. Scott and R. C. Rocha, *Chem.–Eur. J.*, 2011, **17**, 5595; (*t*) T. Kundu, D. Schweinfurth, B. Sarkar, T. K. Mondal, J. Fiedler, S. M. Mobin, V. G. Puranik, W. Kaim and G. K. Lahiri, *Dalton Trans.*, 2012, **41**, 13429.

10 (*a*) S. Roy, B. Sarkar, H. G. Imrich, J. Fiedler, S. Záliš, R. Jiménez-Aparicio, F. A. Urbanos, S. M. Mobin, G. K. Lahiri and W. Kaim, *Inorg. Chem.*, 2012, **51**, 9273; (*b*) H. Agarwala, T. M. Scherer, S. Maji, T. K. Mondal, S. M. Mobin, J. Fiedler, F. A. Urbanos, R. Jiménez-Aparicio, W. Kaim and G. K. Lahiri, *Chem.–Eur. J.*, 2012, **18**, 5667; (*c*) A. Das, T. Scherer, S. Maji, T. K. Mondal, S. M. Mobin, F. A. Urbanos, R. Jiménez-

Dalton Transactions Accepted Manuscript

Aparicio, W. Kaim and G. K. Lahiri, *Inorg. Chem.*, 2011, **50**, 7040; (*d*) S. Patra, B. Sarkar, S. Maji, J. Fiedler, F. A. Urbanos, R. Jiménez-Aparicio, W. Kaim and G. K. Lahiri, *Chem.–Eur. J.*, 2006, **12**, 489; (*e*) S. Kar, B. Sarkar, S. Ghumaan, D. Roy, F. A. Urbanos, J. Fiedler, R. B. Sunoj, R. Jiménez-Aparicio, W. Kaim and G. K. Lahiri, *Inorg. Chem.*, 2005, **44**, 8715; (*f*) S. Patra, B. Sarkar, S. Ghumaan, J. Fiedler, W. Kaim and G. K. Lahiri, *Inorg. Chem.*, 2004, **43**, 6108; (*g*) S. Kar, N. Chanda, S. M. Mobin, A. Datta, F. A. Urbanos, V. G. Puranik, R. Jiménez-Aparicio and G. K. Lahiri, *Inorg. Chem.*, 2004, **43**, 4911; (*h*) S. Patra, T. A. Miller, B. Sarkar, M. Niemeyer, M. D. Ward and G. K. Lahiri, *Inorg. Chem.*, 2003, **42**, 4707.

11 (*a*) P. Mondal, F. Ehret, M. Bubrin, A. Das, S. M. Mobin, W. Kaim and G. K. Lahiri, *Inorg. Chem.*, 2013, **52**, 8467; (*b*) A. Das, T. M. Scherer, S. M. Mobin, W. Kaim and G. K. Lahiri, *Chem.–Eur. J.*, 2012, **18**, 11007; (*c*) A. Das, T. M. Scherer, A. D. Chowdhury, S. M. Mobin, W. Kaim and G. K. Lahiri, *Inorg. Chem.*, 2012, **51**, 1675; (*d*) D. Kumbhakar, B. Sarkar, A. Das, A. K. Das, S. M. Mobin, J. Fiedler, W. Kaim and G. K. Lahiri, *Dalton Trans.*, 2009, 9645; (*e*) D. Kumbhakar, B. Sarkar, S. Maji, S. M. Mobin, J. Fiedler, F. A. Urbanos, R. Jiménez-Aparicio, W. Kaim and G. K. Lahiri, *J. Am. Chem. Soc.*, 2008, **130**, 17575; (*f*) B. Sarkar, S. Patra, J. Fiedler, R. B. Sunoj, D. Janardanan, G. K. Lahiri and W. Kaim, *J. Am. Chem. Soc.*, 2008, **130**, 3532; (*g*) S. Ghumaan, B. Sarkar, S. Maji, V. G. Puranik, J. Fiedler, F. A. Urbanos, R. Jiménez-Aparicio, W. Kaim and G. K. Lahiri, *Chem.–Eur. J.*, 2008, **14**, 10816; (*h*) S. Maji, B. Sarkar, S. M. Mobin, J. Fiedler, F. A. Urbanos, R. Jiménez-Aparicio, W. Kaim and G. K. Lahiri, *Inorg. Chem.*, 2008, **47**, 5204; (*i*) S. Chakraborty, R. H. Laye, P. Munshi, R. L. Paul, M. D. Ward and G. K. Lahiri, *J. Chem. Soc.*, *Dalton Trans.*, 2002, 2348.

Dalton Transactions Accepted Manuscript

12 J. A. Weil, J. R. Bolton and J. E. Wertz, *Electron Paramagnetic Resonance*, Wiley: New York, 1994, p. 532.

13 T. Kundu, A. D. Chowdhury, D. De, S. M. Mobin, V. G. Puranik, A. Datta and G. K. Lahiri, *Dalton Trans.*, 2012, **41**, 4484.

14 A. Das, T. Kundu, S. M. Mobin, J. L. Priego, R. Jiménez-Aparicio and G. K. Lahiri, *Dalton Trans.*, 2013, **42**, 13733.

15 (*a*) S. J. Dickson, S. C. G. Biagini and J. W. Steed, *Chem. Commun.*, 2007, 4955; (*b*) P. D. Beer, *Chem. Commun.*, 1996, 689; (*c*) S. J. Dickson, M. J. Paterson, C. E. Willans, K. M. Anderson and J. W. Steed, *Chem.–Eur. J.*, 2008, **14**, 7296; (*d*) J. G. Vos and J. M. Kelly, *Dalton Trans.*, 2006, 4869; (*e*) S. Derossi, H. Adams and M. D. Ward, *Dalton Trans.*, 2007, 33; (*f*) T. -P. Lin, C. -Y. Chen, Y. -S. Wen and S. -S. Sun, *Inorg. Chem.*, 2007, **46**, 9201; (*g*) M. H. V. Huynh, D. M. Dattelbaum and T. J. Meyer, *Coord. Chem. Rev.*, 2005, **249**, 457; (*h*) F. Szemes, D. Hesek, Z. Chen, S. W. Dent, M. G. B. Drew, A. J. Goulden, A. R. Graydon, A. Grieve, R. J. Mortimer, T. Wear, J. S. Weightman and P. D. Beer, *Inorg. Chem.*, 1996, **35**, 5868; (*i*) P. D. Beer, S. W. Dent and T. J. Wearb, *J. Chem. Soc., Dalton Trans.*, 1996*,* 2341; (*j*) E. Berni, I. Gosse, D. Badocco, P. Pastore, N. Sojic and S. Pinet, *Chem.–Eur. J.*, 2009, **15**, 5145; (*k*) R. Martínez-Máñez and F. Sancenón, *Chem. Rev.*, 2003, **103**, 4419; (*l*) P. D. Beer, F. Szemes, V. Balzani, C. M. Salà, M. G. B. Drew, S. W. Dent and M. Maestri, *J. Am. Chem. Soc.*, 1997, **119**, 11864; (*m*) S. Das, D. Saha, C. Bhaumik, S. Dutta and S. Baitalik, *Dalton Trans.*, 2010, **39**, 4162; (*n*) C. Bhaumik, S. Das, D. Saha, S. Dutta and S. Baitalik, *Inorg. Chem.*, 2010, **49**, 5049; (*o*) C. Bhaumik, S. Das, D. Saha, S. Dutta and S. Baitalik, *Inorg. Chem.*, 2011, **50**,

Dalton Transactions Accepted Manuscript

12586; (*p*) C. Bhaumik, D. Maity, S. Das and S. Baitalik, *Polyhedron*, 2013, **52**, 890; (*q*) D. Maity, C. Bhaumik, D. Mondal and S. Baitalik, *Dalton Trans.*, 2014, **43**,1829.

16 (*a*) A. Bianchi, K. Bowman-James and E. García-Espana, *Supramolecular Chemistry of Anions*, Ed. Wiley-VCH: New York, 1997; (*b*) M. Arunachalam and P. Ghosh, *Org. Lett.*, 2010, **12**, 328; (*c*) F. Zapata, A. Caballero, A. Tarraga and P. Molina, *J. Org. Chem.*, 2010, **75**, 162; (*d*) X. -F. Shang and X. -F. Xu, *Biosystems*, 2009, **96**, 165; (*e*) T. Y. Joo, N. Singh, G. W. Lee and D. O. Jang, *Tetrahedron Lett.*, 2007, **48**, 8846; (f) P. Gamez, T. J. Mooibroek, S. J. Teat and J. Reedijk, *Acc. Chem. Res.*, 2007, **40**, 435; (*g*) F. M. Ashcroft, *Ion Channels and Disease*, Academic Press: San Diego, CA, 2000; (*i*) M. M. Linn, D. C. Poncio and V. G. Machado, *Tetrahedron Lett.*, 2007, **48**, 4547; (*j*) M. Boiocchi, L. Del Boca, D. E. Gomez, L. Fabbrizzi, M. Licchelli and E. Monzani, *J. Am. Chem. Soc.*, 2004, **126**, 16507.

17 (*a*) D. Saha, S. Das, D. Maiti and S. Baitalik, *Indian J. Chem. Sec A*, **50A**, 1418; (*b*) D. Saha, S. Das, D. Maiti, S. Dutta and S. Baitalik, *Inorg. Chem.*, 2011, **50**, 46.

18 (*a*) M. M. Richter, B. Scott, K. J. Brewer and R. D. Willett, *Acta Cryst.*, 1991, **C47**, 2443; (*b*) K. D. Demadis, D. M. Dattelbaum, E. M. Kober, J. J. Concepcion, J. J. Paul, T. J. Meyer and P. S. White, *Inorg. Chim. Acta*, 2007, **360**, 1143; (*c*) S. Ye, B. Sarkar, C. Duboc, J. Fiedler and W. Kaim, *Inorg. Chem.*, 2005, **44**, 2843; (*d*) S. Baitalik, P. Bag, U. Flörke and K. Nag, *Inorg. Chim. Acta*, 2004, **357**, 699; (*e*) S. Das, S. Karmakar, D. Saha and S. Baitalik, *Inorg. Chem.*, 2013, **52**, 6860.

19 (*a*) S. Chakraborty, R. H. Laye, R. L. Paul, R. G. Gonnade, V. G. Puranik, M. D. Ward and G. K. Lahiri, *J. Chem. Soc., Dalton Trans*., 2002, 1172; (*b*) S. Patra, B. Sarkar, S. M. Mobin, W. Kaim and G. K. Lahiri, *Inorg. Chem.*, 2003, **42**, 6469.

Dalton Transactions Accepted Manuscript

20 (*a*) S. Kar, B. Sarkar, S. Ghumaan, M. Leboschka, J. Fiedler, W. Kaim and G. K. Lahiri, *Dalton Trans.*, 2007, 1934; (*b*) S. Ghumaan, S. Mukherjee, S. Kar, D. Roy, M. M. Shaikh, R. B. Sunoj and G. K. Lahiri, *Eur. J. Inorg. Chem.*, 2006, 4426.

21 (*a*) W. Kaim, *Coord. Chem. Rev.*, 1987, **76**, 187; (*b*) E. Waldhör, L. D. Slep, J. Fiedler, J. A. Olabe and W. Kaim, *Inorg. Chem.*, 1997, **36**, 2969; (*c*) M. Wanner, T. Scheiring, L. D. Slep, L. M. Baraldo, J. A. Olabe, S. Záliš, E. J. Baerends and W. Kaim, *Inorg. Chem.*, 2001, **40**, 5704; (*d*) P. H. Rieger, *Electron Spin Resonance*, RSC Publishing: Cambridge, 2007.

22 B. Sarkar, S. Patra, J. Fiedler, R. B. Sunoj, D. Janardanan, S. M. Mobin, M. Niemeyer, G. K. Lahiri and W. Kaim, *Angew. Chem. Int. Ed.*, 2005, **35**, 5655.

23 C. Creutz, *Prog. Inorg. Chem*., 1983, **30**, 1.

24 M. B. Robin and P. Day, *Adv. Inorg. Chem. Radiochem.*, 1967, **10**, 247.

25 (*a*) J. Poppe, M. Moscherosch and W. Kaim, *Inorg. Chem.*, 1993, **32**, 2640; (*b*) S. Chellamma and M. Lieberman, *Inorg. Chem.*, 2001, **40**, 3177; (*c*) S. Patra, B. Sarkar, S. Ghumaan, J. Fiedler, W. Kaim and G. K. Lahiri, *Dalton Trans.*, 2004, 754; (*d*) S. Ghumaan, B. Sarkar, N. Chanda, M. Sieger, J. Fiedler, W. Kaim and G. K. Lahiri, *Inorg. Chem.*, 2006, **45**, 7955; (*e*) W. Kaim, B. Sarkar and G. K. Lahiri, *Spectroelectrochemistry*, RSC Publishing: Cambridge, 2008, p. 68.

26 (*a*) V. Balzani, N. Sabbatini and F. Scandola, *Chem. Rev.*, 1986, **86**, 319; (*b*) S. O. Kang, D. Powell, V. W. Day and K. Bowman-James, *Angew. Chem. Int. Ed.*, 2006, **45**, 1921; (*c*) I. G. Shenderovich, P. M. Tolstoy, N. S. Golubev, S. N. Smirnov, G. N. Denisov and H. -H. Limbach, *J. Am. Chem. Soc.*, 2003, **125**, 11710; (*d*) M. A. Rampi, M. T. Indelli, F. Scandola, F. Pina and A. J. Parola, *Inorg. Chem.*, 1996, **35**, 3355.

Dalton Transactions Accepted Manuscript

27 (*a*) T. Kundu, S. M. Mobin and G. K. Lahiri, *Dalton Trans.*, 2010, **39**, 4232; (*b*) Y. Cui, H. -J. Mo, J. -C. Chen, Y. -L. Niu, Y. -R. Zhong, K. -C. Zheng and B. -H. Ye, *Inorg. Chem.*, 2007, **46**, 6427; (*c*) Y. Liu, B. -H. Han and Y. -T. Chen, *J. Phys. Chem. B*, 2002, **106**, 4678; (*d*) Y. Liu, B. -H. Han, S. -X. Sun, T. Wada and Y. Inoue, *J. Org. Chem.*, 1999, **64**, 1487; (*e*) C. Basu, S. Biswas, A. P. Chattopadhyay, H. S. Evans and S. Mukherjee, *Eur. J. Inorg. Chem.*, 2008, 4927; (*f*) L. Wang, X. -J. Zhu, W. -Y. Wong, J. -P. Guo, W. -K. Wong, and Z. -Y. Li, *Dalton Trans.*, 2005, 3235; (*g*) B. Valeur, J. Pouget, J. Bourson, M. Kaschke and N. P. Ernsting, *J. Phys. Chem.*, 1992, **96**, 6545; (*h*) Y. Liu, B. Li, T. Wada and Y. Inoue, *J. Org. Chem.*, 2001, **66**, 225.

28 D. Saha, S. Das, C. Bhaumik, S. Dutta and S. Baitalik, *Inorg. Chem.*, 2010, **49**, 2334.

29 (*a*) D. F. Shriver and P. W. Atkins, *Inorganic Chemistry*, Ed. III Oxford University Press: 1999; (*b*) T. D. B. Morgan, G. Stedman and P. A. E. Whincup, *J. Chem.* Soc., 1965, 4813; (*c*) T. I. Crowell and M. G. Hankins, *J. Phys. Chem.*, 1969, **73**, 1380.

30 S. Ghosh, A. R. Choudhury, T. N. G. Row and U. Maitra, *Org. Lett.*, 2005, **7**, 1441.

31 (*a*) Y. Cui, Y. -L. Niu, M. -L. Cao, K. Wang, H. -J. Mo, Y. -R. Zhong and B. -H. Ye, *Inorg. Chem.*, 2008, **47**, 5616; (*b*) H. -J. Mo, Y. -L. Niu, M. Zhang, Z. -P. Qiao and B. -H. Ye, *Dalton Trans.*, 2011, **40**, 8218.

32 (*a*) J. Wang, F. -Q. Bai, B. -H. Xia, L. Sun and H. -X. Zhang, *J. Phys. Chem. A*, 2011, **115**, 1985; (*b*) M. Sarkar, R. Yellampalli, B. Bhattacharya, R. K. Kanaparthi and A. Samanta, *J. Chem. Sci.*, 2007, **119**, 91; (*c*) D. W. Kim, J. Kim, J. Hwang, J. K. Park and J. S. Kim, *Bull. Korean Chem. Soc*., 2012, **33**, 1159; (*d*) T. Ghosh and B. G. Maiya, *J. Phys. Chem. A*, 2004, **108**, 11249.

33 P. A. Lay, A. M. Sargeson and H. Taube, *Inorg. Synth.*, 1986, **24**, 291.

Dalton Transactions Accepted Manuscript

34 (*a*) G. M. Sheldrick, *Acta Crystallogr*., *Sect. A: Fundam. Crystallogr*., 2008, **64**, 112; (*b*) *Program for Crystal Structure Solution and Refinement*, University of Göttingen, Göttingen, Germany, 1997.

35 M. J. Frisch, G. W. Trucks, H. B. Schlegel, G. E. Scuseria, M. A. Robb, J. R. Cheeseman, G. Scalmani, V. Barone, B. Mennucci, G. A. Petersson, H. Nakatsuji, M. Caricato, X. Li, H. P. Hratchian, A. F. Izmaylov, J. Bloino, G. Zheng, J. L. Sonnenberg, M. Hada, M. Ehara, K. Toyota, R. Fukuda, J. Hasegawa, M. Ishida, T. Nakajima, Y. Honda, O. Kitao, H. Nakai, T. Vreven, J. A. Montgomery, J. E. Peralta Jr., F. Ogliaro, M. Bearpark, J. J. Heyd, E. Brothers, K. N. Kudin, V. N. Staroverov, R. Kobayashi, J. Normand, K. Raghavachari, A. Rendell, J. C. Burant, S. S. Iyengar, J. Tomasi, M. Cossi, N. Rega, J. M. Millam, M. Klene, J. E. Knox, J. B. Cross, V. Bakken, C. Adamo, J. Jaramillo, R. Gomperts, R. E. Stratmann, O. Yazyev, A. J. Austin, R. Cammi, C. Pomelli, J. W. Ochterski, R. L. Martin, K. Morokuma, V. G. Zakrzewski, G. A. Voth, P. Salvador, J. J. Dannenberg, S. Dapprich, A. D. Daniels, O. Farkas, J. B. Foresman, J. V. Ortiz, J. Cioslowski and D. J. Fox, *Gaussian 09* (Revision A.02): Gaussian, Inc., Wallingford CT 2009.

36 (*a*) D. Andrae, U. Haeussermann, M. Dolg, H. Stoll and H. Preuss, *Theor. Chim. Acta*, 1990, **77**, 123; (*b*) P. Fuentealba, H. Preuss, H. Stoll and L. V. Szentpaly, *Chem. Phys. Lett.*, 1989, **89**, 418.

37 (*a*) R. Bauernschmitt and R. Ahlrichs, *Chem. Phys. Lett.*, 1996, **256**, 454; (*b*) R. E. Stratmann, G. E. Scuseria and M. J., Frisch, *J. Chem. Phys.* 1998, **109**, 8218; (*c*) M. E. Casida, C. Jamorski, K. C. Casida and D. R. Salahub, *J. Chem. Phys.*, 1998, **108**, 4439.

Dalton Transactions Accepted Manuscript

38 (*a*) V. Barone and M. Cossi, *J. Phys. Chem. A*, 1998, **102**, 1995; (*b*) M. Cossi and V. Barone, *J. Chem. Phys.*, 2001, **115**, 4708; (*c*) M. Cossi, N. Rega, G. Scalmani and V. Barone, *J. Comput. Chem.*, 2003, **24**, 669.

39 S. Leonid, *Chemissian 1.7*, 2005−2010. Available at http://www.chemissian.com

40 D. A. Zhurko and G. A. Zhurko, *Chemcraft 1.5*, Plimus: San Diego, CA. Availaible at http://www.chemcraftprog.com

Dalton Transactions Accepted Manuscript

Table 1 Selected crystallographic parameters of **1**

Compound	[**1**]·3H_2O
Formula	$C_{31}H_{28}N_8O_5Os$
M_r	782.81
Radiation	CuK_α
Crystal system	Monoclinic
Space group	P 21/c
a/Å	9.535(5)
b/Å	25.768(5)
c/Å	12.599(5)
α (°)	90.000(5)
β (°)	93.582(5)
γ (°)	90.000(5)
V/Å^3	3089(2)
μ/mm^{-1}	4.181
Z	4
T/K	150(2)
ρ_{calcd}/g cm^{-3}	1.683
F(000)	1544
θ range (°)	3.91 to 72.43
Data/restraints/parameters	6058 / 16 / 415
R1, wR2 ($I>2\sigma(I)$)	0.0194, 0.0512
R1, wR2 (all data)	0.0198, 0.0516
GOF on F^2	0.881
Largest diff. peak per hole/e Å^{-3}	0.711 and -0.973

Dalton Transactions Accepted Manuscript

Table 2 Experimental (X-ray) and DFT calculated bond distances (Å) and bond angles (°) of **1**

	X-ray	DFT		X-ray	DFT
	1 (*S*=0)	**1** (*S*=0)		**1** (*S*=0)	**1** (*S*=0)
Bond distances (Å)			Bond angles (Å)		
Os1-N5	2.042(2)	2.068	N6-Os1-N8	96.17(8)	100.03
Os1-N6	2.046(2)	2.071	N6-Os1-N7	89.54(9)	96.70
Os1-N7	2.022(2)	2.054	N8-Os1-N7	78.76(8)	78.01
Os1-N8	2.046(2)	2.053	N8-Os1-N1	89.15(8)	89.31
Os1-N1	2.059(2)	2.068	N7-Os1-N1	95.92(8)	96.21
Os1-O1	2.116(18)	2.090	N6-Os1-N5	78.27(8)	77.84
N1-C3	1.328(3)	1.353	N6-Os1-O1	97.46(8)	90.25
N1-C2	1.385(3)	1.381	N7-Os1-O1	171.66(7)	169.18
N2-C4	1.357(3)	1.368	N1-Os1-O1	77.47(8)	78.01
N2-C3	1.344(3)	1.331	N5-Os1-O1	88.25(7)	87.44
N3-C5	1.328(3)	1.323	N8-Os1-N5	173.49(8)	177.87
N3-C11	1.396(3)	1.379	N6-Os1-N1	173.04(8)	165.38
N4-C5	1.354(3)	1.380	N7-Os1-N5	97.66(8)	102.08
N4-C6	1.380(3)	1.374	N8-Os1-O1	95.90(8)	92.65
C6-C11	1.397(3)	1.423	O1-C1-O2	122.3(2)	121.62
C1-C2	1.461(3)	1.473	N8-Os1-N1	89.15(8)	89.31
C2-C4	1.397(3)	1.406	N7-Os1-N1	95.92(8)	96.21
C4-C5	1.458(3)	1.456	N6-Os1-N5	78.27(8)	77.84
C1-O1	1.299(3)	1.325	N6-Os1-O1	97.46(8)	90.25
C1-O2	1.246(3)	1.238			
C6-C7	1.400(3)	1.397			
C7-C8	1.390(4)	1.393			
C8-C9	1.391(4)	1.411			
C9-C10	1.390(4)	1.391			
C10-C11	1.394(3)	1.403			

Dalton Transactions Accepted Manuscript

Table 3 Electrochemical data[a] of **1** and [**2**](ClO$_4$)$_2$

Complex	$E°_{298}$/ V(ΔE_p/mV)				K_{c1} (between Ox1 and Ox2)	K_{c2} (between Red1 and Red2)
	Ox1	Ox2	Red1	Red2		
1	0.23 (110)	-	-1.51(80)	-1.80(90)	-	8.2×10^4
[**2**](ClO$_4$)$_2$	0.24 (60)	0.50 (60)	-1.52 (60)	-1.80 (90)	2.5×10^4	5.5×10^4

[a] From cyclic voltammetry in CH_3CN/ 0.1 mol dm^{-3} [Et_4N][ClO_4] at 100 mV s^{-1}. Potential in V *versus* SCE; peak potential difference ΔE_p/mV (in parentheses).

Dalton Transactions Accepted Manuscript

Table 4 DFT calculated selected MO compositions for $\mathbf{1}^n$ and $\mathbf{2}^n$

Complex (spin state)	MO	Fragments	% Composition
1 (*S*=0)	HOMO	HL/Os	88/12
	LUMO	bpy	92
$\mathbf{1}^-$ (*S*=1/2)	SOMO	bpy	89
	α-LUMO	bpy	81
$\mathbf{1}^{2-}$ (*S*=1)	SOMO 1	bpy	80
	SOMO 2	bpy	91
$\mathbf{2}^{4+}$ (*S*=1)	β-LUMO	HL/Os	16/70
$\mathbf{2}^{3+}$ (*S*=1/2)	β-HOMO	HL/Os	15/71
	β-LUMO	HL/Os	11/72
$\mathbf{2}^{2+}$ (*S*=0)	HOMO	HL/Os	15/65
	LUMO	bpy	95
$\mathbf{2}^{+}$ (*S*=1/2)	SOMO	bpy	92
	α-LUMO	bpy	91
2 (*S*=1)	SOMO 1	bpy	94
	SOMO 2	bpy	94

Dalton Transactions Accepted Manuscript

Table 5 Mulliken spin density values of $\mathbf{1}^n$ (n = +1, -1, -2) and $\mathbf{2}^n$ (n = 0, +1, +3, +4) using UB3LYP

Complex	Os	HL^{2-}	bpy
$\mathbf{1}^+$ (S=1/2)	0.220	0.878	-0.016
$\mathbf{1}^-$ (S=1/2)	-0.096	0	1.097
$\mathbf{1}^{2-}$ (S=1)	0.261	0.008	1.620
$\mathbf{2}^{3+}$ (S=1/2)	0.887(Os1),0.005(Os2)	0.117	-0.003
$\mathbf{2}^{4+}$ (S=1)	0.915(Os1),0.811(Os2)	0.275	0.011
$\mathbf{2}^+$ (S=1/2)	0.002(Os1), -0.046(Os2)	0.004	1.046
2 (S=1)	-0.074(Os1), -0.071(Os2)	0.005	2.139

Dalton Transactions Accepted Manuscript

Table 6 Experimental and TD-DFT (B3LYP/CPCM/CH_3CN) calculated electronic transitions for $\mathbf{1}^n$ (n = 0, +1) and $\mathbf{2}^n$ (n = +2, +3, +4)

λ/nm (exp) (ε/dm^{3}mol^{-1}cm^{-1})	λ/ nm (DFT)	f	Transition	Character
$\mathbf{1}^+$ (S=1/2)				
399(6280)	397	0.0334	(43%)HOMO-2(α)→LUMO+1(α) (19%)HOMO-2(α)→LUMO+1(α)	Os(dπ)→bpy(π*) Os(dπ)→bpy(π*)
342(20980)	339	0.1924	(52%)HOMO-12(β)→LUMO(β)	$HL^{\bullet-}$(π)→ $HL^{\bullet-}$(π*)
313(27080)	334	0.2821	(43%) HOMO-12(β)→LUMO(β) (41%)SOMO(α)→LUMO+6(α)	$HL^{\bullet-}$(π)→ $HL^{\bullet-}$(π*) $HL^{\bullet-}$(π)→ $HL^{\bullet-}$(π*)
288(26750)	281	0.1399	(20%)HOMO-6(α)→LUMO+1(α) (20%) SOMO(α)→LUMO+12(a)	$HL^{\bullet-}$(π)→bpy(π*) $HL^{\bullet-}$(π)→$HL^{\bullet-}$(π*)
255(25290)	272	0.1318	(25%) HOMO-20(β)→LUMO(β) (21%) HOMO-19(β)→LUMO(β)	$HL^{\bullet-}$(π)→$HL^{\bullet-}$(π*) bpy(π)→ $HL^{\bullet-}$(π*)
1 (S=0)				
720(1740)	653	0.0075	(55%)HOMO→LUMO	HL^{2-}(π)→bpy(π*)
518(6680)	496	0.0651	(59%)HOMO-2→LUMO+1	Os(dπ)→bpy(π*)
405(9230)	382	0.2097	(27%)HOMO-1→LUMO+3 (26%)HOMO→LUMO+4	HL^{2-}(π)→bpy(π*) HL^{2-}(π)→bpy(π*)
330(20440)	359	0.3900	(49%)HOMO-1→LUMO+6 (23%)HOMO→LUMO+6	HL^{2-}(π)→bpy(π*) HL^{2-}(π)→bpy(π*)
298(45370)	278	0.1861	(44%)HOMO-7→LUMO+1 (18%)HOMO→LUMO+7	HL^{2-}(π)→bpy(π*) HL^{2-}(π)→bpy(π*)
248(25710)	239	0.0804	(59%)HOMO-7→LUMO+2	HL^{2-}(π)→bpy(π*)
$\mathbf{2}^{4+}$ (S=1)				

Dalton Transactions Accepted Manuscript

507(3120)	539	0.0016	(93%)HOMO-9(β)→LUMO(β)	HL^{2-}(π)→Os(dπ)
477(3340)	482	0.0067	(89%)HOMO-10(β)→LUMO(β)	bpy(π)→Os(dπ)
350(22620)	341	0.0270	(53%)HOMO-2(β)→LUMO+6(β)	HL^{2-}(π)→ HL^{2-}(π*)
318(47630)	304	0.0276	(29%)HOMO-11(α)→LUMO(α) (28%)HOMO-9(α)→LUMO(α)	bpy(π)→bpy(π*) bpy(π)→bpy(π*)
307(50620)	296	0.0408	(40%)HOMO-5(α)→LUMO+4(α) (25%)HOMO-7(β)→LUMO+3(β)	bpy(π)→HL^{2-}(π*) bpy(π)→bpy(π*)
278(52740)	291	0.0595	(24%)HOMO-7(β)→LUMO+5(β) (24%)HOMO-2(β)→LUMO+8(β)	bpy(π)→bpy(π*) HL^{2-}(π)→bpy(π*)
252(58820)	266	0.0716	(35%)HOMO-1(β)→LUMO+12(β) (21%)HOMO-2(β)→LUMO+12(β)	HL^{2-}(π)→bpy(π*) HL^{2-}(π)→bpy(π*)
$\mathbf{2}^{3+}$ (*S*=1/2)				
Not resolved	1360	0.0093	(91%)HOMO-1(β)→LUMO(β)	Os(dπ)→Os(dπ)
621(2990)	593	0.0031	(70%)SOMO(α)→LUMO+2(α) (69%)HOMO(β)→LUMO+2(β)	Os(dπ)/HL^{2-}(π)→bpy(π*) Os(dπ)→bpy(π*)
504(10170)	482	0.0155	(84%)HOMO-2(α)→LUMO+1(α)	Os(dπ)→bpy(π*)
399(14650)	421	0.0152	(91%)HOMO-12(β)→LUMO(β)	bpy(π)→Os(dπ)
322(35170)	321	0.0899	(30%)HOMO-3(β)→LUMO+6(β) (29%)HOMO-3(α)→LUMO+4(α)	HL^{2-}(π)→bpy(π*) HL^{2-}(π)→bpy(π*)
296(76340)	277	0.2724	(46%)HOMO-7(β)→LUMO+4(β) (43%)HOMO-7(β)→LUMO+3(β)	bpy(π)→bpy(π*) bpy(π)→bpy(π*)
248(55140)	262	0.0823	(33%)HOMO-9(α)→LUMO+5(α) (15%)HOMO-9(α)→LUMO+6(α)	bpy(π)→bpy(π*) bpy(π)→bpy(π*)
$\mathbf{2}^{2+}$ (*S*=0)				
689(5230)	625	0.0069	(61%)HOMO→LUMO+1	Os(dπ)→bpy(π*)
514(18470)	479	0.0827	(46%)HOMO-2→LUMO+3	Os(dπ)→bpy(π*)
			(24%)HOMO-1→LUMO+1	Os(dπ)→bpy(π*)
360(22580)	361	0.0703	(45%)HOMO-6→LUMO+2	HL^{2-}(π)→bpy(π*)
297(97470)	301	0.2174	(50%)HOMO-6→LUMO+4	HL^{2-}(π)→bpy(π*)

Dalton Transactions Accepted Manuscript

248(55460)	232	0.1092	(42%)HOMO-8→LUMO+9 (23%)HOMO-8→LUMO+11	$HL^{2-}(\pi)\rightarrow bpy(\pi^*)$ $HL^{2-}(\pi)\rightarrow bpy(\pi^*)$

Figure captions

Fig. 1 ORTEP diagram of **1**. Hydrogens and solvent of crystallisation are removed for clarity. Ellipsoids are drawn at 50% probability level.

Fig. 2 Cyclic voltammograms of **1** (green) and [**2**]$(ClO_4)_2$ (red) in CH_3CN/ 0.1 mol dm^{-3} $[Et_4N][ClO_4]$ at 298 K. Scan rate: 100 mV s^{-1} (oxidation couples are only shown).

Fig. 3 DFT calculated Mulliken spin density plots of $\mathbf{1}^n$ (n= +1,-1,-2) and $\mathbf{2}^n$ (n= +4,+3,+1,0).

Fig. 4 EPR spectrum of $\mathbf{1}^+$ in CH_3CN at 77 K.

Fig. 5 UV-vis-NIR spectroelectrochemical plots for the conversions of (a) $\mathbf{1}\rightarrow\mathbf{1}^+$, (b) $\mathbf{2}^{2+}\rightarrow\mathbf{2}^{3+}$ and (c) $\mathbf{2}^{3+}\rightarrow\mathbf{2}^{4+}$ (10^{-4} mol dm^{-3}) on sequential additions of $(NH_4)_2Ce(NO_3)_6$ (CAN) solution (10^{-3} mol dm^{-3}) in CH_3CN.

Fig. 6 The visual change in colour of **1** ($5x10^{-5}$ mol dm^{-3}) in CH_3CN on addition of one equivalent of the TBA salt of the anions, F^-, Cl^-, Br^-, I^-, OAc^-, SCN^-, HSO_4^-, $H_2PO_4^-$.

Fig. 7 UV-vis. spectral changes of **1** (5 x 10^{-5} mol dm^{-3}) in CH_3CN on addition of eight equivalents TBA salts of Cl^-, Br^-, I^-, OAc^-, SCN^-, HSO_4^-, $H_2PO_4^-$ and one equivalent of F^-.

Dalton Transactions Accepted Manuscript

Fig. 8 UV-vis spectral changes of **1** ($5x10^{-5}$ mol dm^{-3}) in CH_3CN on gradual additions of up to one equivalent of [TBA][F]. The inset shows the changes in absorbances at 518 nm and 545 nm for **1** as a function of the equivalents of F^-.

Fig. 9 Changes in the cyclic voltammograms (oxidation couple only) of **1** and $\mathbf{2}^{2+}$ (10^{-3} mol dm^{-3}) in CH_3CN upon gradual additions of TBAF up to one equivalent.

Fig. 10 ^{1}H-NMR titration of **1** in $CDCl_3$ in presence of TBA salt of F^- ion (0-1 equivalent).

Dalton Transactions Accepted Manuscript

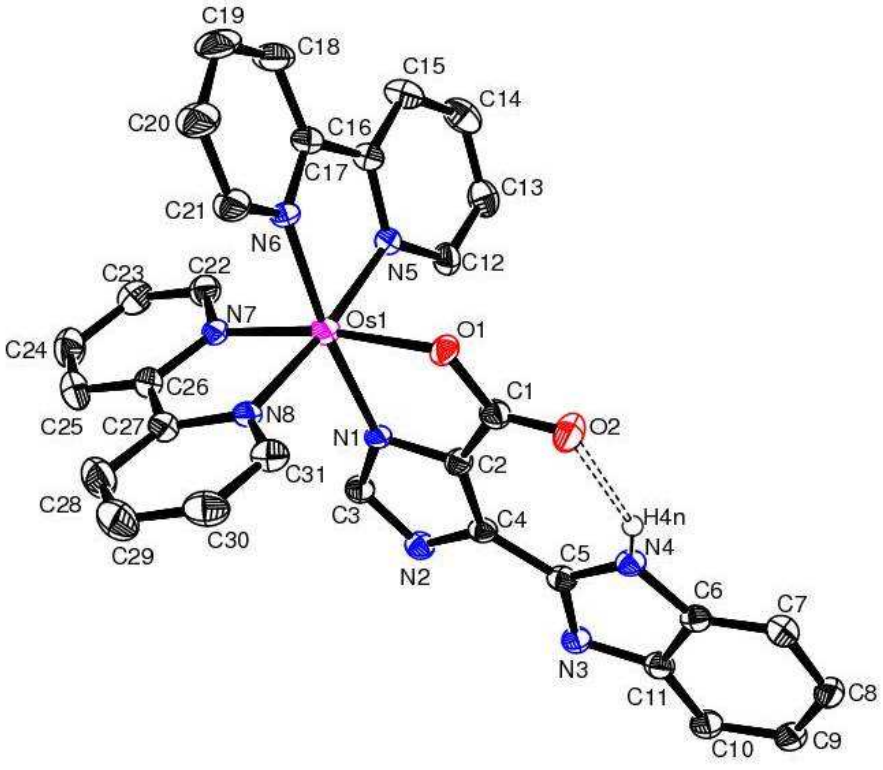

Fig. 1

Dalton Transactions Accepted Manuscript

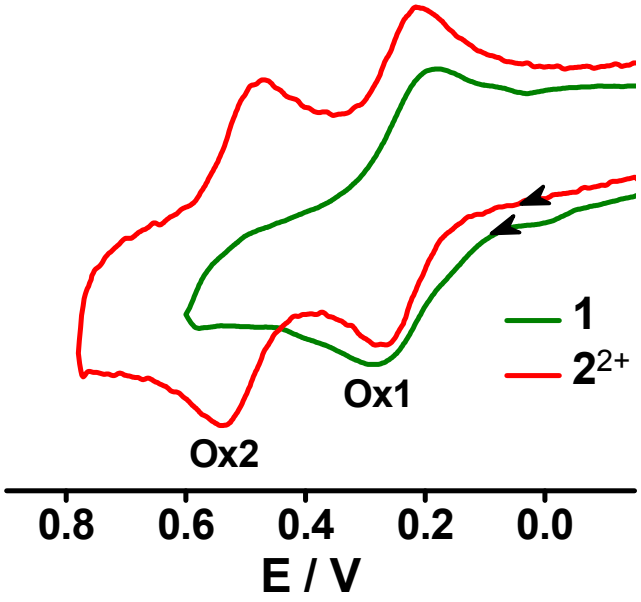

Fig. 2

Dalton Transactions Accepted Manuscript

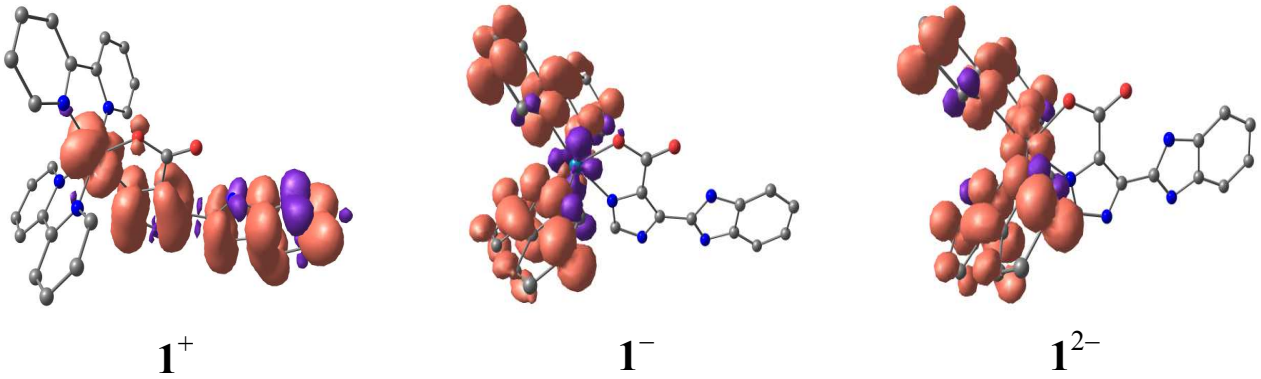

$\mathbf{1}^{+}$ $\mathbf{1}^{-}$ $\mathbf{1}^{2-}$

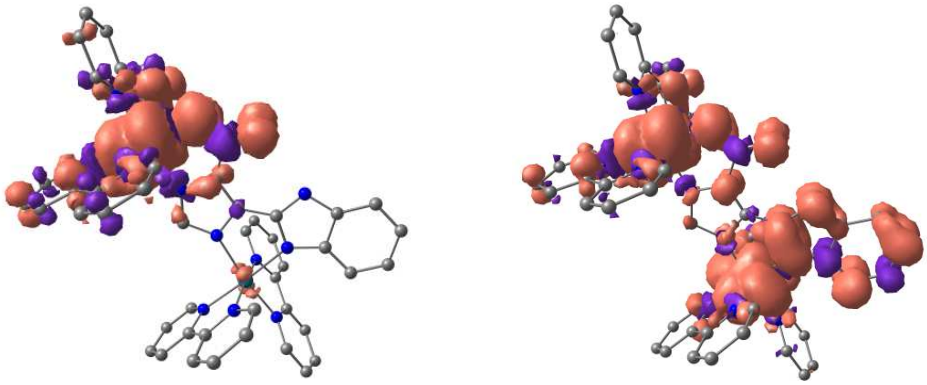

$\mathbf{2}^{3+}$ $\mathbf{2}^{4+}$

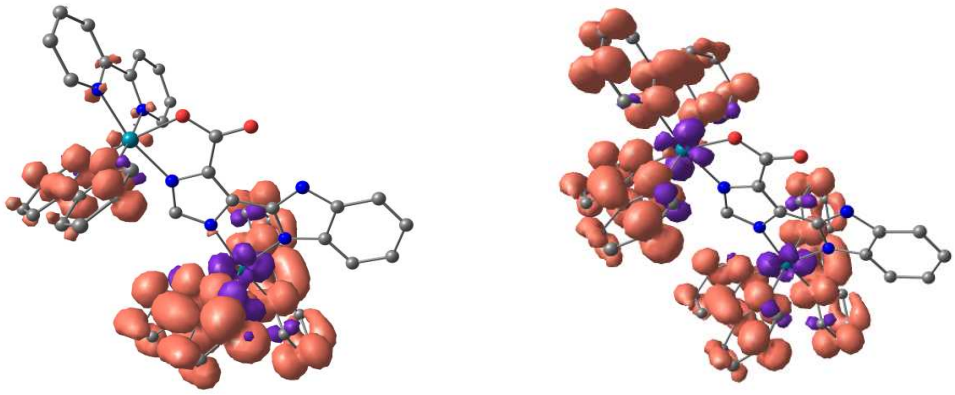

$\mathbf{2}^{+}$ $\mathbf{2}$

Fig. 3

Dalton Transactions Accepted Manuscript

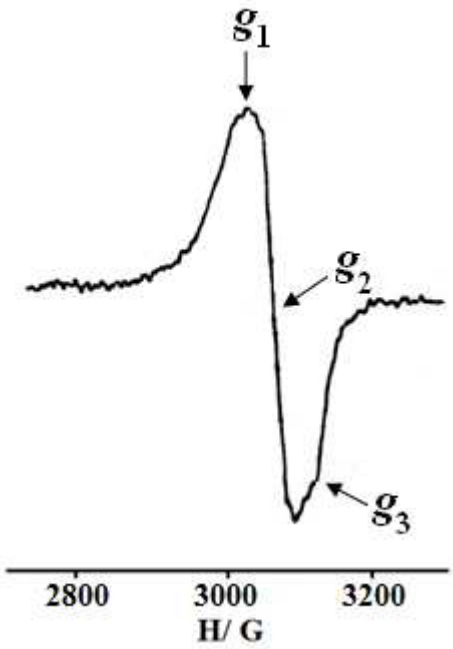

Fig. 4

Dalton Transactions Accepted Manuscript

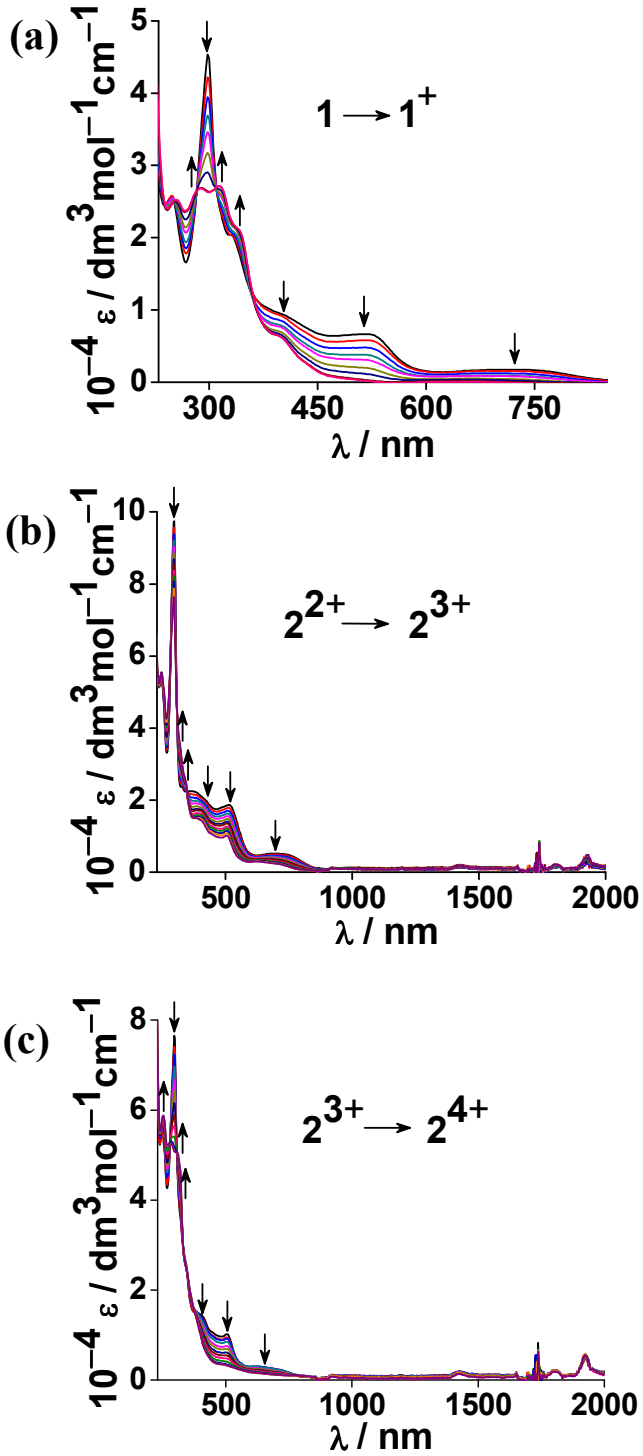

Fig. 5

Dalton Transactions Accepted Manuscript

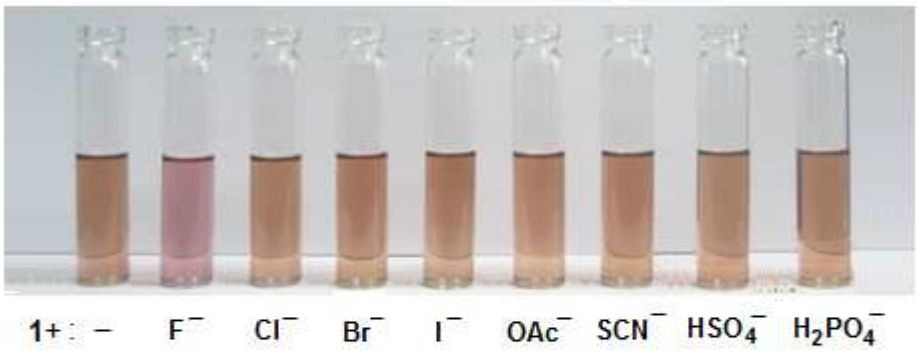

Fig. 6

Dalton Transactions Accepted Manuscript

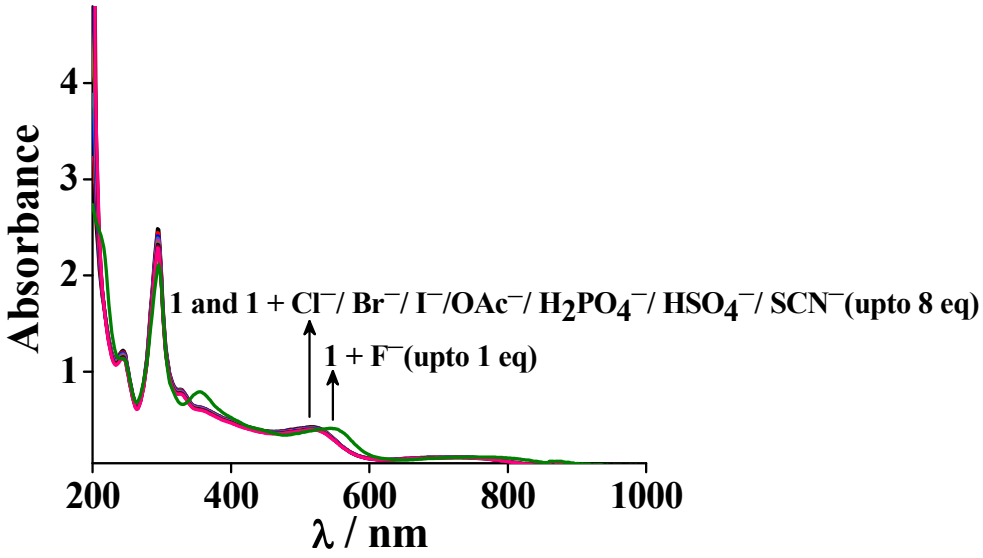

Fig. 7

Dalton Transactions Accepted Manuscript

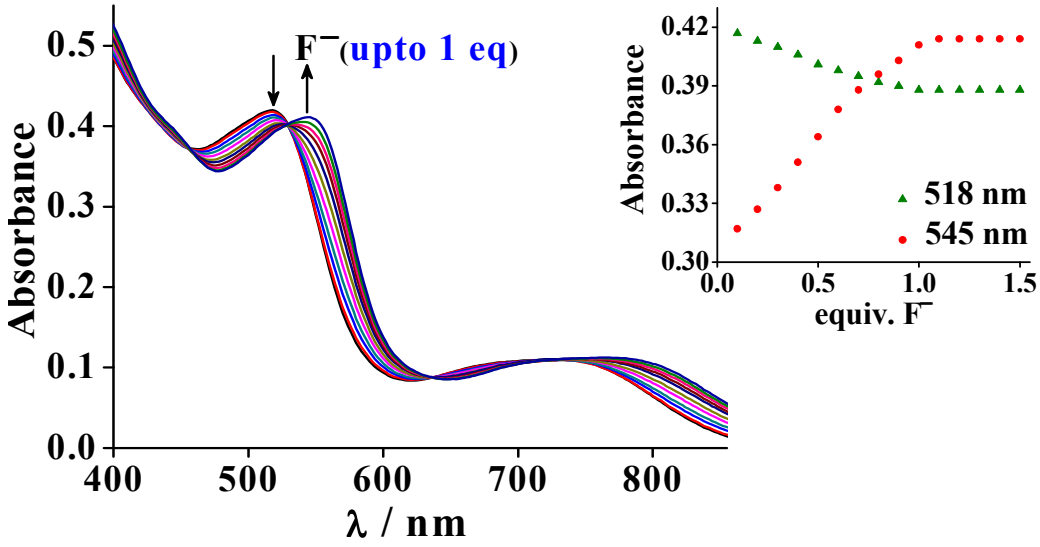

Fig. 8

Dalton Transactions Accepted Manuscript

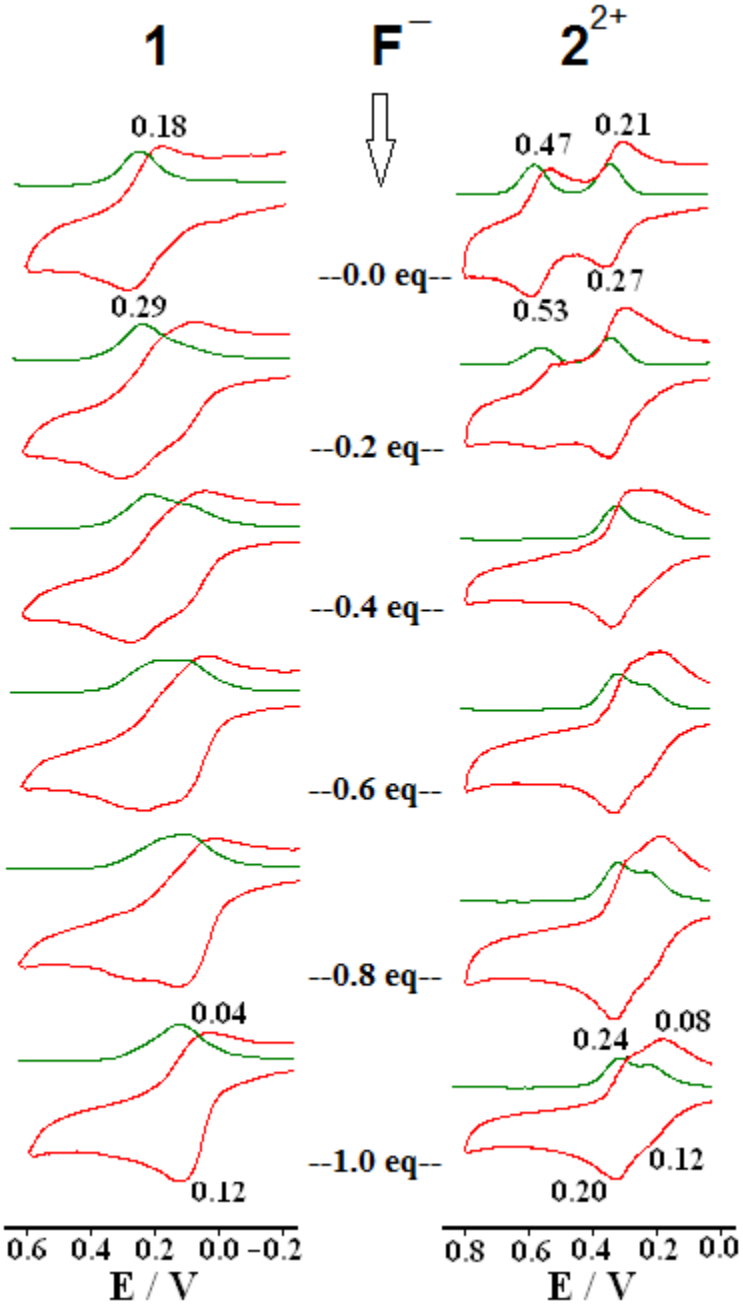

Fig. 9

Dalton Transactions Accepted Manuscript

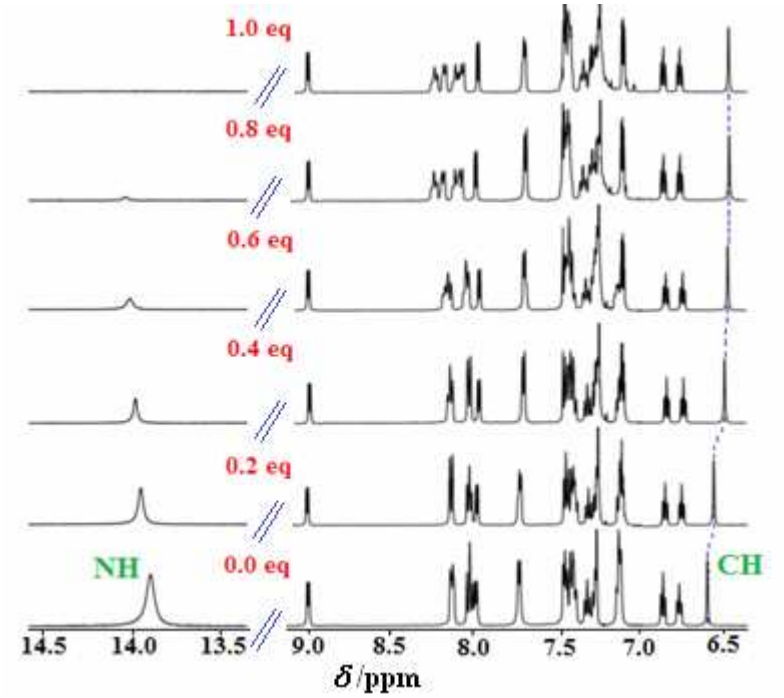

Fig. 10

Dalton Transactions Accepted Manuscript

Dalton Transactions Accepted Manuscript

Electronic structures and selective fluoride sensing features of $Os(bpy)_2(HL^{2-})$ and $[\{Os(bpy)_2\}_2(\mu\text{-}HL^{2-})]^{2+}$ (H_3L: 5-(1*H*-benzo[*d*]imidazol-2-yl)-1*H*-imidazole-4-carboxylic acid)

Ankita Das,[a] Hemlata Agarwala,[a] Tanaya Kundu,[a] Prabir Ghosh,[a] Sudipta Mondal,[a] Shaikh M Mobin,[b] and Goutam Kumar Lahiri*[a]

[a]*Department of Chemistry, Indian Institute of Technology Bombay, Powai, Mumbai-400076, India. E-mail: lahiri@chem.iitb.ac.in*

[b]*Discipline of Chemistry, School of Basic Sciences, Indian Institute of Technology Indore, Indore 452017, India*

The noninnocence of coordinated HL^{2-} in $[(bpy)_2Os(HL^{2-})]^n$ (**1**^{n}) and (**2**^{n}) and their selectivity towards F^- recognition have been evaluated.

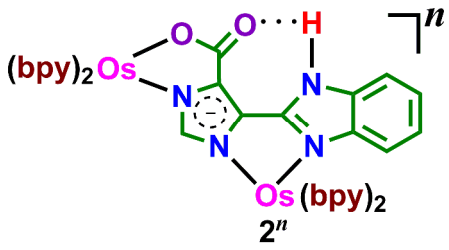

2^n

Dalton Transactions Accepted Manuscript